Cell

Neural mechanism underlying depressive-like state associated with social status loss

Graphical abstract

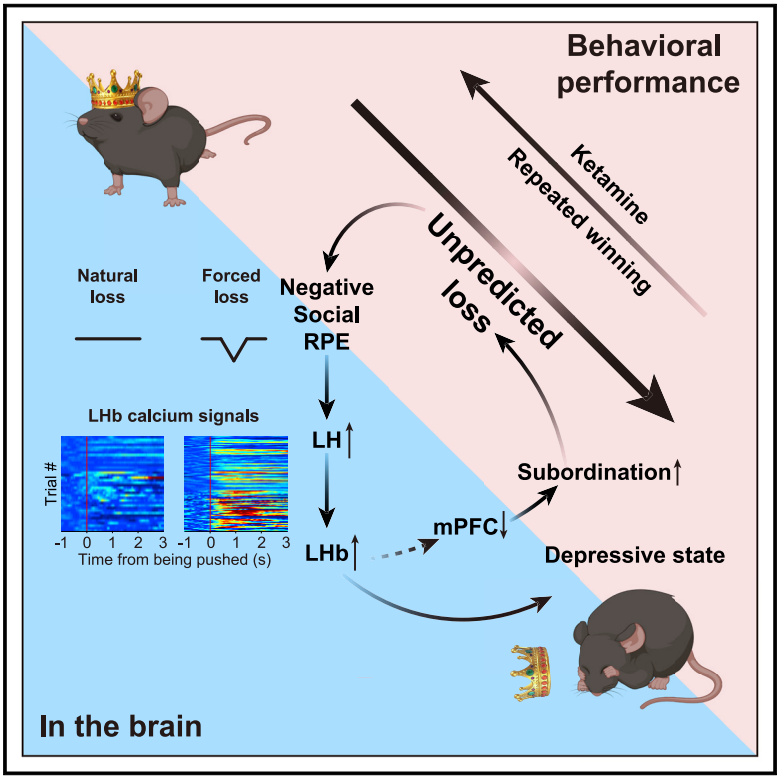

Highlights

- Forced loss lowers social ranks and induces depressive-like behaviors
- Forced loss generates negative reward prediction error
- Forced loss but not natural loss activates LH-LHb circuit and induces LHb bursting
- LHb burst firing inhibits mPFC and reinforces subordination

Authors

Zhengxiao Fan, Jiarui Chang, Yilan Liang, ..., Ying Xu, Qi-Jing Li, Hailan Hu

Correspondence

huhailan@zju.edu.cn

In brief

A psychological and non-violent behavioral paradigm is developed and used to understand the neural mechanisms behind depressive-like behaviors following a decline in social status.

Fan et al., 2023, Cell *186*, 1–17
February 2, 2023
https://doi.org/10.1016/j.cell.2022.12.033

CellPress

Please cite this article in press as: Fan et al., Neural mechanism underlying depressive-like state associated with social status loss, Cell (2023), https://doi.org/10.1016/j.cell.2022.12.033

Cell

CellPress

Article

Neural mechanism underlying depressive-like state associated with social status loss

Zhengxiao Fan,[1,2] Jiarui Chang,[2] Yilan Liang,[2] Hong Zhu,[2] Chaoyi Zhang,[2] Diyang Zheng,[2] Junying Wang,[2] Ying Xu,[2] Qi-Jing Li,[3] and Hailan Hu[1,2,4,5,6,*]

[1]Department of Neurobiology, Affiliated Mental Health Center & Hangzhou Seventh People's Hospital, Zhejiang University School of Medicine, Hangzhou 310058, China

[2]Liangzhu Laboratory, MOE Frontier Science Center for Brain Science and Brain-Machine Integration, State Key Laboratory of Brain-Machine Intelligence, Zhejiang University, Hangzhou 311121, China

[3]Institute of Molecular and Cell Biology (IMCB) & Singapore Immunology Network (SIgN), Agency for Science, Technology and Research (A*STAR), Singapore 138668, Singapore

[4]Center for Brain Science and Brain-Inspired Intelligence, Guangdong-Hong Kong-Macao Greater Bay Area, Guangzhou 510515, China

[5]Research Units of Brain Mechanisms Underlying Emotion and Emotion disorders, Chinese Academy of Medical Sciences, Beijing 100730, China

[6]Lead contact

*Correspondence: huhailan@zju.edu.cn

https://doi.org/10.1016/j.cell.2022.12.033

SUMMARY

Downward social mobility is a well-known mental risk factor for depression, but its neural mechanism remains elusive. Here, by forcing mice to lose against their subordinates in a non-violent social contest, we lower their social ranks stably and induce depressive-like behaviors. These rank-decline-associated depressive-like behaviors can be reversed by regaining social status. *In vivo* fiber photometry and single-unit electrophysiological recording show that forced loss, but not natural loss, generates negative reward prediction error (RPE). Through the lateral hypothalamus, the RPE strongly activates the brain's anti-reward center, the lateral habenula (LHb). LHb activation inhibits the medial prefrontal cortex (mPFC) that controls social competitiveness and reinforces retreats in contests. These results reveal the core neural mechanisms mutually promoting social status loss and depressive behaviors. The intertwined neuronal signaling controlling mPFC and LHb activities provides a mechanistic foundation for the crosstalk between social mobility and psychological disorder, unveiling a promising target for intervention.

INTRODUCTION

The majority of stresses leading to depression in humans are known to be of social origin.[1] Among them, loss of social status is a particularly prominent risk factor for depressive illness across species.[2,3] Status loss in men increases the risk of depression 3- to 4-fold,[4–6] which becomes even more prominent in the wake of the mental health crisis sparked by the COVID-19 pandemic.[7] In monkeys or chimpanzees, loss of social status is well known to precipitate depressive-like behaviors.[8,9] In domestic hens, while low-ranking hens show mild depressive-like behaviors, a severe and life-threatening depressive-like state was found in alpha birds who fall from high status.[10] Even in lizards or fish, loss of rank or territory may lead to behavioral inhibition suggestive of depression.[11–14] Such prevalence suggests that a phylogenetically conserved mechanism is shared between humankind and animals that account for depression or depressive-like behavioral patterns induced by loss of social status. However, the neural mechanism underlying this profound social-psychological phenomenon has been largely unexplored in mammalian species due to the lack of a suitable animal model. Why is loss of rank, rather than the stable low rank, particularly potent in inducing depressive-like behavior? How does this mental-stress-induced depression mechanistically relate to physical-stress-induced depression? And what is the nature of the neural signals that lead to depressive-like behaviors during status decline? With this information, we can hopefully prevent the depressive-like state resulting from the plunge of social status.

The evolutionary conservation of depression as a result of loss of social status strongly suggests the depressive state serves a function. According to an evolutionary psychology theory, namely, the social competition hypothesis, the depressive state is an adaptation that reinforces yielding behaviors for losers to reduce the cost of social confrontation.[2,15] Therefore, depressive-like behaviors can promote the acceptance of the newly established status quo and have an advantage for the individuals. However, there have been few experiments directly testing this hypothesis. Also, the neural mechanism linking depressive state to yielding behaviors is unknown.

Please cite this article in press as: Fan et al., Neural mechanism underlying depressive-like state associated with social status loss, Cell (2023), https://doi.org/10.1016/j.cell.2022.12.033

The lateral habenula (LHb) has recently been implicated in the pathophysiology of major depression induced by various kinds of physical stress.[16,17] As an anti-reward center, the LHb is activated by a variety of aversive stimuli[18–24] and can inhibit reward-related dopaminergic and serotonergic neurons.[25–27] In a depressive-like state induced by physical stress, such as repeated restraint, footshock, or chemical drugs, the LHb becomes hyperactive,[28–31] showing increased synaptic efficacy, excitability, and burst firing.[19,32,33] However, it has remained unclear whether, apart from physical stress, mental stress such as loss of social status may also activate the LHb to induce a depressive state.

Here, using the dominance tube test, an assay measuring social hierarchy in mice,[34,35] we have developed a paradigm of status loss. This paradigm does not involve any intense physical fights or injuries, but induces depressive-like behaviors in descending mice, with high success rates. Based on this paradigm, and using a combination of *in vivo* electrophysiology recording, fiber photometry, and optogenetic and pharmacological manipulations, we have studied the behavioral changes and activity patterns of the LHb during the hierarchy reorganization.

RESULTS

"Forced loss" paradigm induces a stable loss of social rank

Investigating the mechanistic relationship between social status and depressive-like behaviors, we first ranked C57BL/6J mice using the dominance tube test[34,36,37] and assessed their depressive-like phenotypes after tube test ranks became stable (Figure S1A). We found that tube test ranks did not correlate with performance in the forced swimming test (FST, measuring "behavioral despair") or sucrose preference test (SPT, measuring "anhedonia") (Figures S1B–S1D), suggesting that ranks in a stable hierarchy are not a strong predictor of depressive-like behaviors.

We then asked whether depressive-like behaviors may be associated with a change, especially a downward shift, of social status. For that, we established the "forced loss" paradigm to induce social status loss in mice (Figure 1A). After acquiring a stable tube test rank in groups of four mice, we forced the most dominant (rank 1) mice to lose to their subordinate cagemates (rank 2, 3, and 4) by blocking the subordinate's side of the tube.[38,39] Because there was no way to back out, subordinates could only push forward against the previous rank1 to exit the tube (Video S1). After repeating this procedure 10 trials per day for 4 days, the status of previous rank1 mice stably fell to the bottom (Figure 1B). The forces applied to subordinate mice during their retreats, which were measured by a dynamometer connected to the tube blocker, correlated with the duration of each forced loss trial (Figures S1E–S1G) and gradually decreased (Figure 1C), suggesting less resistance and easier yielding from the original rank1 mice over time. Indeed, frame-by-frame video analysis[37,40] revealed a dramatic change in rank1's coping strategy and behavioral pattern in the tube test after forced loss, with much fewer pushes, more retreats, and less resistance in response to being pushed (Figures 1D, 1E, and S1H–S1J).

The subordinate state after the forced loss in the tube test was also generalized to other forms of competition such as the competition for a warm spot on an ice-cold floor[40] (Figures 1F and S1K). While the original occupation duration of the warm spot correlated with tube test ranks as previously reported[40] (Figure 1F), after forced loss in the tube test, mice significantly decreased their occupation duration and ranks in the warm spot test (Figure 1G). In addition, the loss generalized to other social subjects: as revealed by inter-cage tube test competitions[41] (see STAR Methods), mice after being forced to lose against their own cagemates also showed a significant decrease in winning against mice from other cages (Figure 1H). As a control, rank1 mice that went through the tube without opponents 10 trials per day for 4 days ("go-through-tube" group) showed no significant difference in both warm spot test and inter-cage tube test (Figures 1G and 1H). These results suggest that forced loss leads to a generalized subordinate state.

Throughout the forced loss procedure, no significant differences were detected in fights or other aggressive behaviors, compared with regular tube test encounters. Immediately following the forced loss procedure, we closely monitored the social interactions in the homecage for 15 min with videotaping. "Chasing" or "fighting" behaviors were not significantly different from those after regular tube tests (Figure S1L). However, "staying alone" and "being chased" behaviors were significantly increased after forced loss, compared with either rank1 mice before the forced loss or with rank4 mice after the natural loss (Figure 1I; Video S2).

Forced loss but not natural loss induces depressive-like behaviors in previously dominant mice

To investigate the effect of status loss on depressive-like behaviors, we conducted FST and SPT on mice after the forced loss procedure (Figure 2A). Compared with mice in the naive group, the forced loss individuals showed significantly increased immobile duration and decreased latency to immobility in the FST (Figures 2B and S2A), and decreased sucrose preference in the SPT (Figure 2C). General locomotion, as measured by the open field test, was not affected (Figure S2B). Notably, 14 days after forced loss, the immobile duration in the FST was still significantly higher than that of the control group (Figure 2D). To exclude the effect of possible social transmission of stress,[42] we also tested the cagemates of the forced loss mice and found no such change (Figure S2C). To determine whether the depressive-like behaviors were caused by the loss itself, we included a "natural loss" group of rank1 mice, which were accustomed to loss to more dominant opponents from other cages, and rank4 mice (Figure S2D; see STAR Methods). These mice had an expectation to lose. To further exclude the effect of non-social-related stress during forced loss, we also performed a "mechanical forced loss" control by using a stopper instead of a mouse counterpart to induce the loss (Figures S2E–S2H). These mice had no expectations about the outcome, so none of these two situations were expected to trigger an error signal. After 10 losses per day for 4 days, neither the natural loss nor "mechanical forced loss" groups showed depressive-like behaviors (Figures 2B, 2C, S2D, S2I, and S2J). Collectively, these data

Please cite this article in press as: Fan et al., Neural mechanism underlying depressive-like state associated with social status loss, Cell (2023), https://doi.org/10.1016/j.cell.2022.12.033

CellPress

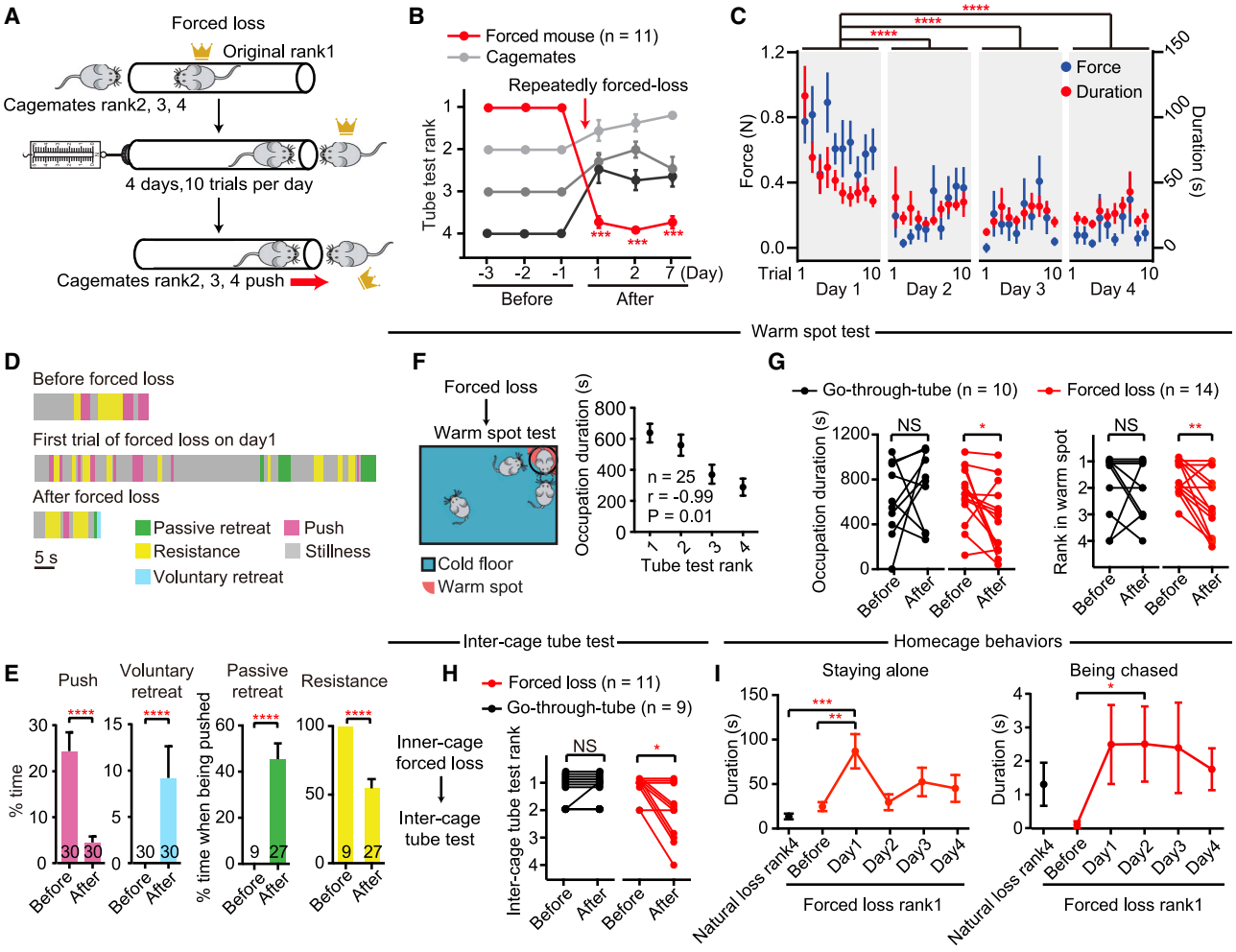

Figure 1. "Forced loss" paradigm induces a stable loss of social rank

(A) Schematic of the "forced loss" paradigm.

(B) Daily tube test results of mice before and after the 4-day forced loss procedure.

(C) Scatterplot showing average forces (blue dots) and durations (red dots) of each forced loss trial during the 4-day procedure.

(D) Sample behavior annotations of an original rank1 mouse in a tube test competition before and after the paradigm and during the first trial of forced loss. The annotation starts when the two mice meet and ends when one mouse is out of the tube. Different colors represent different behavioral epochs. Scale bars, 5 s.

(E) Percentage of time that mice displayed pushes and voluntary retreats during the whole test; percentage of time that mice displayed passive retreats and resistances when being pushed before and after the "forced loss" paradigm. The number of trials is indicated in each bar.

(F) Schematic of the experiments (left) and correlation between occupation duration in the warm spot test and tube test rank (right).

(G) Occupation duration (left) and rank (right) in the warm spot test before and after go-through-tube (black) and forced loss (red).

(H) Left, schematic of the experiments. Right, inter-cage tube test ranks before and after go-through-tube (black) and forced loss (red).

(I) "Staying alone" and "being chased" behaviors in the homecage after regular natural loss and before and after forced loss.

*p < 0.05; **p < 0.01; ***p < 0.001; ****p < 0.0001; ns, not significant. Data are represented as mean ± SEM. See also Figure S1 and Videos S1 and S2.

suggest that it is not losing per se but rather the unpredicted component of losing that may be critical in triggering depressive-like behaviors.

By analyzing factors contributing to the severity of depressive-like behaviors (Figures 2E–2H), we found that the immobile duration in the FST significantly correlated with the average duration of forced loss trials (Figure 2E). There was also a tendency for the FST immobile duration to correlate with the average force (Figure 2F) and the number of days the original rank1 mouse had maintained its dominant position before the forced loss protocol (Figures 2G and 2H). Therefore, the efforts during forced loss and the previous history of dominance may contribute to the severity of a depressive-like phenotype.

Moreover, the depressive-like behaviors induced by forced loss were reversed by the rapid antidepressant drug ketamine,[43] as measured by both the FST and SPT at 1 h after ketamine injection (Figures 2I–2K), illustrating the predictive validity of this model for depression.

Please cite this article in press as: Fan et al., Neural mechanism underlying depressive-like state associated with social status loss, Cell (2023), https://doi.org/10.1016/j.cell.2022.12.033

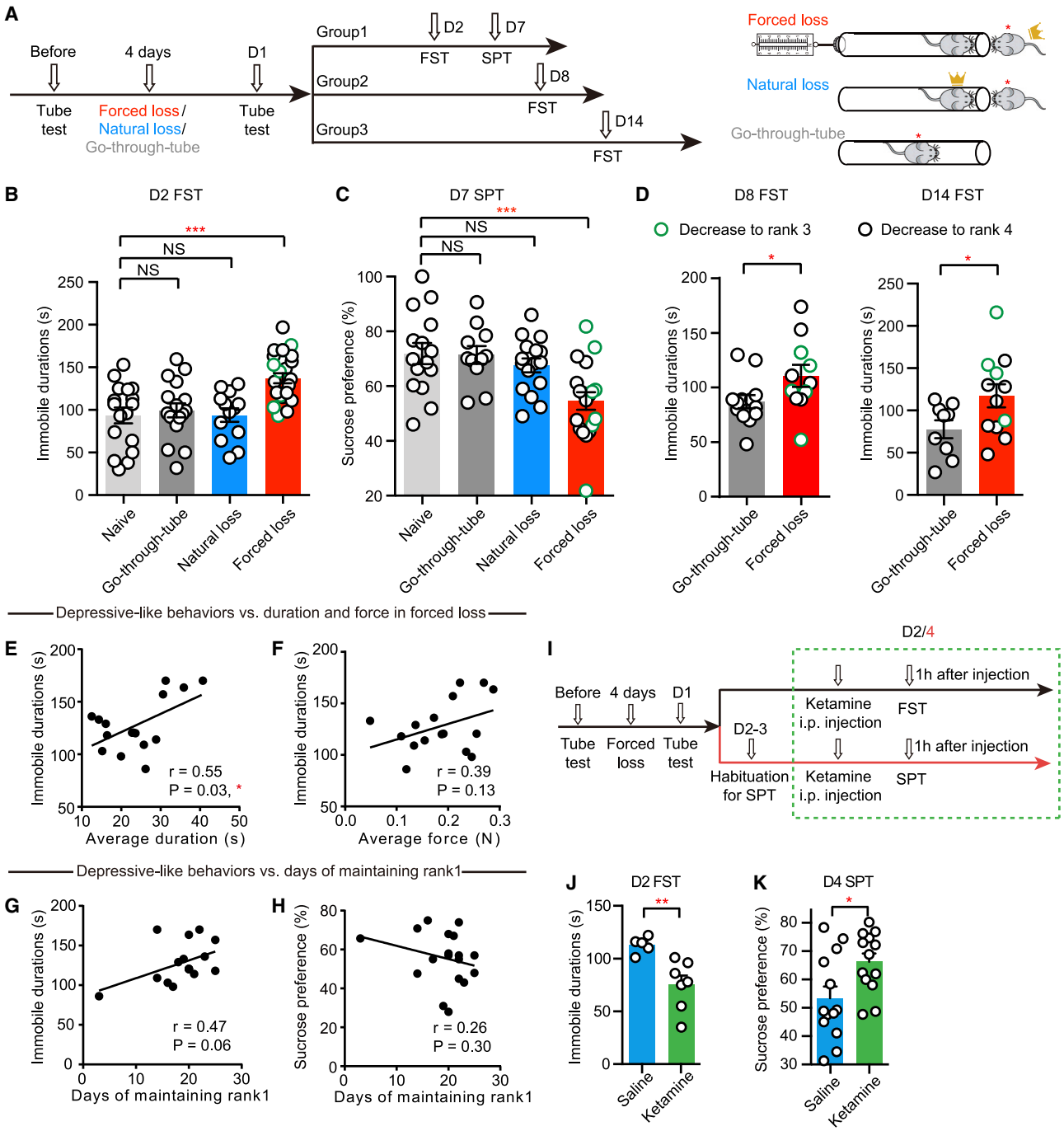

Figure 2. Forced loss but not natural loss induces depressive-like behaviors in previously dominant mice

(A) Experimental paradigm for conducting various behavioral tests (left) and schematic illustration of forced loss, natural loss, and go-through-tube control (right). The red star marks manipulated mice.

(B–D) Immobility in the FST conducted on the 2nd (B), 8th, and 14th day (D); sucrose preference in the SPT on the 7th day (C) after naive control, 4-day go-through-tube, natural loss, and forced loss procedures. Individuals decreasing to rank3 and rank4 in the forced loss group are indicated by green and black dots, respectively.

(E–H) Scatterplots showing the correlation between average duration (E) or force (F) of forced trials and immobility in the FST, as well as between depressive-like behaviors in the FST (G) or SPT (H), and the number of days that the forced mouse had maintained rank1 before the forced loss protocol.

(I) Experimental schedule for ketamine injection experiment.

(J and K) Depressive-like behaviors after forced loss were rapidly reversed by ketamine i.p. injection 1 h before test.

*p < 0.05; **p < 0.01; ***p < 0.001; ns, not significant. Data are represented as mean ± SEM. See also Figure S2.

Please cite this article in press as: Fan et al., Neural mechanism underlying depressive-like state associated with social status loss, Cell (2023), https://doi.org/10.1016/j.cell.2022.12.033

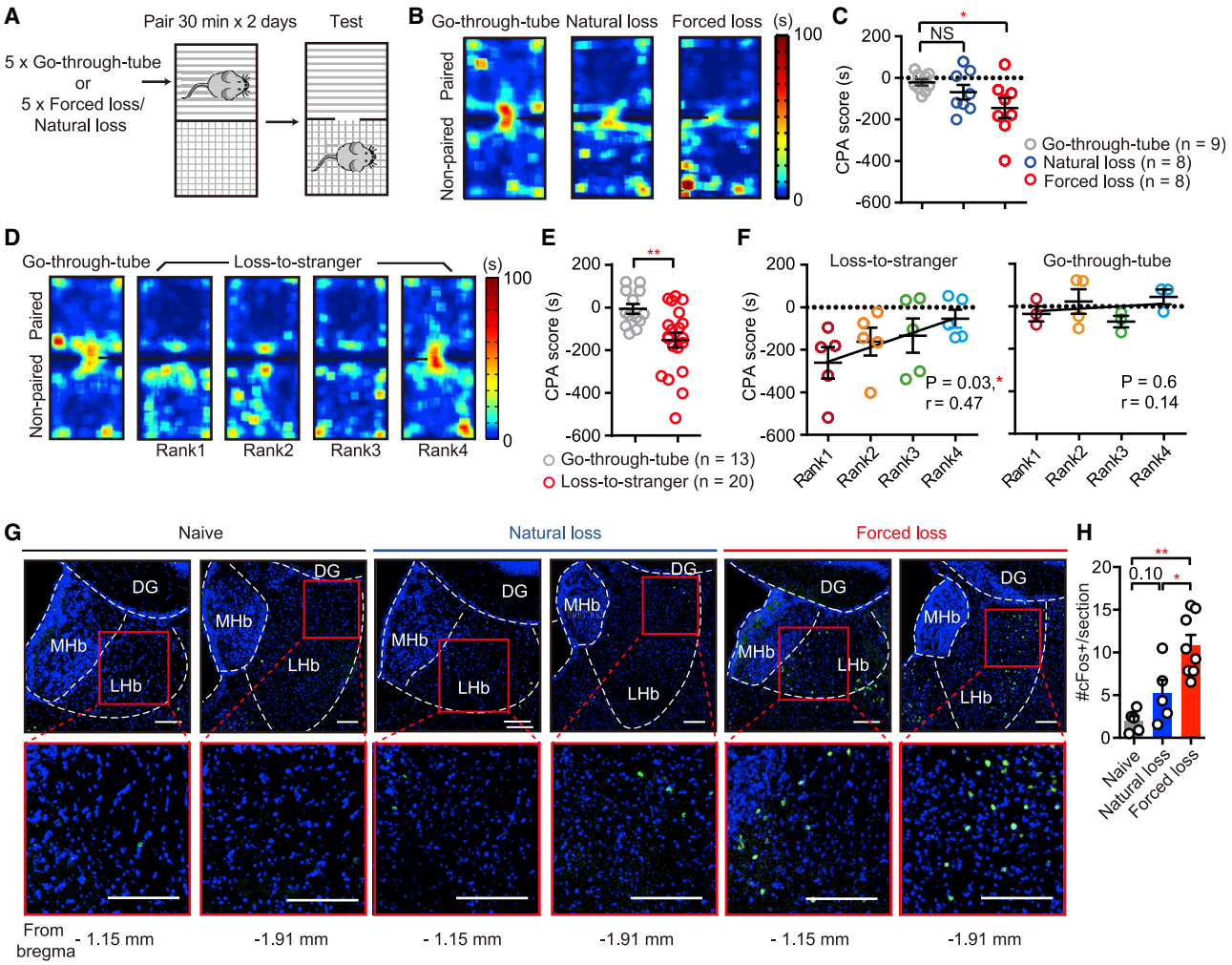

Figure 3. Forced loss induces a negative reinforcing effect and c-Fos activation in the LHb

(A) Behavioral paradigm of CPA of rank1 mice after either go-through-tube, natural loss, or forced loss.

(B–E) (B and D) Example heatmaps showing exploration time during test trials of rank1 mice after 2-day conditioned pairing under three pairing conditions (B) or go-through-tube and loss-to-stranger experience (D). Black lines demarcate individual zones in the CPA apparatus. 5 mice in each rank position were tested for loss-to-stranger. (C and E) Quantitation of CPA scores in (B) and (D).

(F) Correlation of CPA score with mouse rank.

(G) Representative images of c-Fos IHC signals in the LHb in naive control (left), after 10 trials of natural loss (middle) and forced loss (right). Green, c-Fos; blue, Hoechst. Scale bars, 100 μm.

(H) Quantification of total c-Fos$^+$ cells in the LHb.

*p < 0.05; **p < 0.01; ns, not significant. Data are represented as mean ± SEM.

Forced loss induces a negative reinforcing effect and activates LHb neurons

The different outcomes of forced loss versus natural loss led us to hypothesize that defeat by previous inferior opponents may induce a social-related negative reward prediction error (RPE) (a discrepancy between the expectation of winning and the reality of losing) signal. As a negative RPE signal should negatively reinforce behavior—e.g., direct behavior away from associated stimuli—we subjected mice to a conditioned place avoidance test (CPA), pairing mice to one of the two chambers immediately after five natural or forced loss trials (Figure 3A, see STAR Methods). If mice were in a negative-valenced state, they would later tend to avoid the chamber associated with this state.[44] Compared with mice going through the tube, mice paired after forced loss, but not natural loss, spent significantly less time in the paired chamber during the test phase, as reflected in the negative CPA score (Figures 3B and 3C), indicating that unexpected loss caused an aversive state. Moreover, we also made mice of different ranks lose to unfamiliar mice (strangers) before the CPA pairing and found that their average CPA scores positively correlated with their tube test ranks (Figures 3D–3F). This indicates that mice at higher ranks are more vulnerable to losing, compared with mice at lower ranks that may have adapted better to the experience of losing.

Please cite this article in press as: Fan et al., Neural mechanism underlying depressive-like state associated with social status loss, Cell (2023), https://doi.org/10.1016/j.cell.2022.12.033

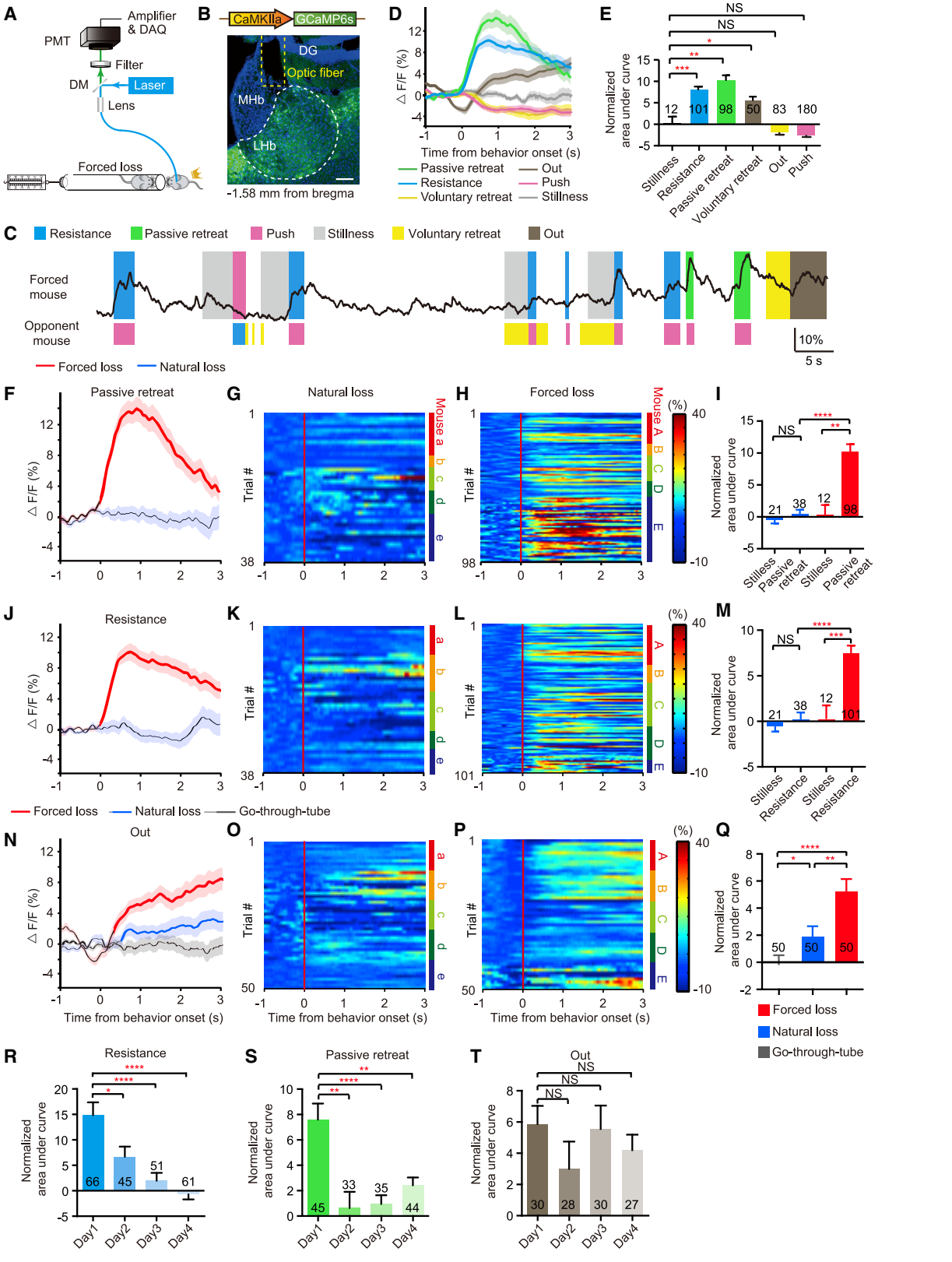

(legend on next page)

Please cite this article in press as: Fan et al., Neural mechanism underlying depressive-like state associated with social status loss, Cell (2023), https://doi.org/10.1016/j.cell.2022.12.033

Since LHb has been implicated in the coding of aversive emotional stimuli,[18–24] we examined the immunohistochemistry (IHC) signal of c-Fos, a marker of neural excitation,[45–47] in the LHb. Although the natural loss group showed a trend of increase, compared with naive mice, the forced loss group showed significantly more c-Fos signals in the LHb (Figures 3G and 3H).

LHb and its upstream input encode negative social prediction errors during forced loss

To understand how LHb neural activities dynamically change during forced loss, we used adeno-associated virus (AAV) with CaMKIIa promoter to express the calcium indicator GCaMP6s in the LHb of stable rank1 mice and installed optic fibers above the LHb for *in vivo* photometry recordings during the forced loss (Figures 4A, 4B, and S3A). Alignment of calcium signals with the video-annotated behavioral epochs in the tube test revealed that LHb neurons were excited in three types of epochs: "resistance" and "passive retreat", both of which were associated with pushes from the opponents, as well as "out", indicating the moment of loss (Figures 4C–4E; Video S3). By contrast, "push" and "voluntary retreat" epochs did not elicit such increase in calcium signals (Figures 4C–4E and S3B).

We next compared these calcium signals with those induced by going through the tube or by natural loss. Strikingly, the LHb calcium signals, as measured by area under the curve (AUC), induced by opponent pushes in the "resistance" and "passive retreat" epochs were only apparent in the forced loss but not the natural loss group (Figures 4F–4M and S3C). The "out-of-tube"-induced increase in LHb calcium signals was also much larger in the forced loss group (Figures 4N–4Q and S3C). These results indicate that LHb neurons are strongly activated by negative RPE induced by unexpected pushes from previously subordinate opponents or by unexpected loss to these subordinates.

Prediction errors should be modifiable by experience and decrease with repetition. Indeed, the AUC of calcium transients induced by opponent pushes in the "resistance" and "passive retreat" epochs decreased over the 4 days of forced loss (Figures 4R and 4S). Interestingly, the calcium transients from the "out" epochs showed no such decrease over days (Figure 4T), indicating that the aversive feelings accompanying the moment of loss do not decay within this period.

Next, we tried to identify the upstream input to the LHb that may convey the negative RPE signal during forced loss (Figure S4). Among the major upstream inputs to the LHb, two inputs have been strongly implicated in dominance-related behaviors, the medial prefrontal cortex (mPFC) and lateral hypothalamus (LH).[21,40,48] To test the contribution of each of these two input pathways in the forced-loss-induced RPE encoding, we injected AAVretro-hSyn-Cre into the LHb and AAV-CAG-Flex-GCaMP6s into the mPFC or the LH and then monitored calcium signals in the LHb-projecting neurons during natural and forced losses (Figures S4A, S4B, S4F, and S4G). Only LHb-projecting neurons in the LH, but not the mPFC (Figures S4H–S4J), were specifically activated by unexpected loss but not natural loss (Figures S4C–S4E), suggesting that the LH-LHb pathway may specifically encode the prediction error during forced loss.

Forced loss induces LHb activation and burst firing

Since LHb activation, in particular its burst firing, signifies a depressive-like state induced by physical stressors,[32,33,49,50] we asked whether mental stress, such as forced loss, may also increase LHb activity and burst firing. Exploring this, a custom-made 16-channel platiniridium single electrode was implanted in the LHb of rank1 mice to record single-unit neural activities *in vivo* during forced loss (Figures 5A, 5B, and S5A–S5C). Consistent with the photometry recording, analysis of single-unit activity during the tube test revealed that despite response heterogeneity, there were more neurons activated in the "being pushed" (including both "resistance" and "passive retreat") epochs during forced but not natural loss trials (Figures S5D–S5K). Notably, right after the first forced trial, and over the 10 trials of forced loss on day 1, recorded LHb units showed a dramatic increase in activity, especially in the burst firing mode (Figures 5C and 5D). Tonic firing was also acutely enhanced, although to a lesser extent (Figure S5L). When recorded at 30 min after returning mice to the homecages, burst firing, but not tonic firing, continued to show a significant increase, as revealed by pairwise comparison of multiple unit activities before and after forced loss (Figure S5M). Over the 4-day forced loss

Figure 4. LHb encodes negative social prediction error during forced loss

(A) Schematic illustrating the fiber photometry setup for recording LHb neuron calcium activity during forced loss.

(B) Illustration of the viral injection site, viral expression, and optic fiber placement (indicated by the yellow dotted line) in the LHb, the boundary of which is outlined by the white dotted line. Green, GCaMP6s; blue, Hoechst. MHb, medial habenula; DG, dentate gyrus. Scale bars, 100 μm.

(C) Example trace of LHb calcium signal and behavioral epochs of forced mouse (top) and behavioral epochs of the opponent (bottom) during day 1 of forced loss. Scale bars, 10% delta F/F, 5 s.

(D) Averaged post-stimulus histograms (PSTHs) of the delta F/F ratio of LHb calcium signals aligned to various detailed behavioral epochs during day 1 of forced loss.

(E) Bar chart showing the normalized AUC during various detailed behavioral epochs, compared with stillness throughout day 1 of forced loss. The number of trials is indicated in each bar.

(F–Q) (F, J, and N) Averaged PSTHs of the delta F/ F ratio of calcium signals aligned to passive retreat (F), resistance (J), and out (N) during day 1 of forced loss (red shade), natural loss (blue shade), or go-through-tube (gray shade). Thick black lines indicate the mean and colored shaded areas indicate the SEM. Red or blue segments indicate statistically significant increases from the baseline ($p < 0.05$, multivariate permutation test). (G, H, K, L, O, and P) Heatmap representations of the delta F/ F ratio of calcium signals aligned to the passive retreat (G and H), resistance (K and L), and out (O and P) during day 1 of natural loss (G, K, and O) and forced loss (H, L, and P). Color bars at the right of each heatmap represent different individual mice. (I, M, and Q) Normalized AUC of LHb calcium signals for stillness, passive retreat (I), resistance (M), and out (Q) during different procedures.

(R–T) Normalized AUC of LHb calcium signals for the same behavioral epochs across 4 training days. The number of trials is indicated in each bar.

*$p < 0.05$; **$p < 0.01$; ***$p < 0.001$; ****$p < 0.0001$; ns, not significant. Data are represented as mean ± SEM. See also Figures S3 and S4 and Video S3.

Please cite this article in press as: Fan et al., Neural mechanism underlying depressive-like state associated with social status loss, Cell (2023), https://doi.org/10.1016/j.cell.2022.12.033

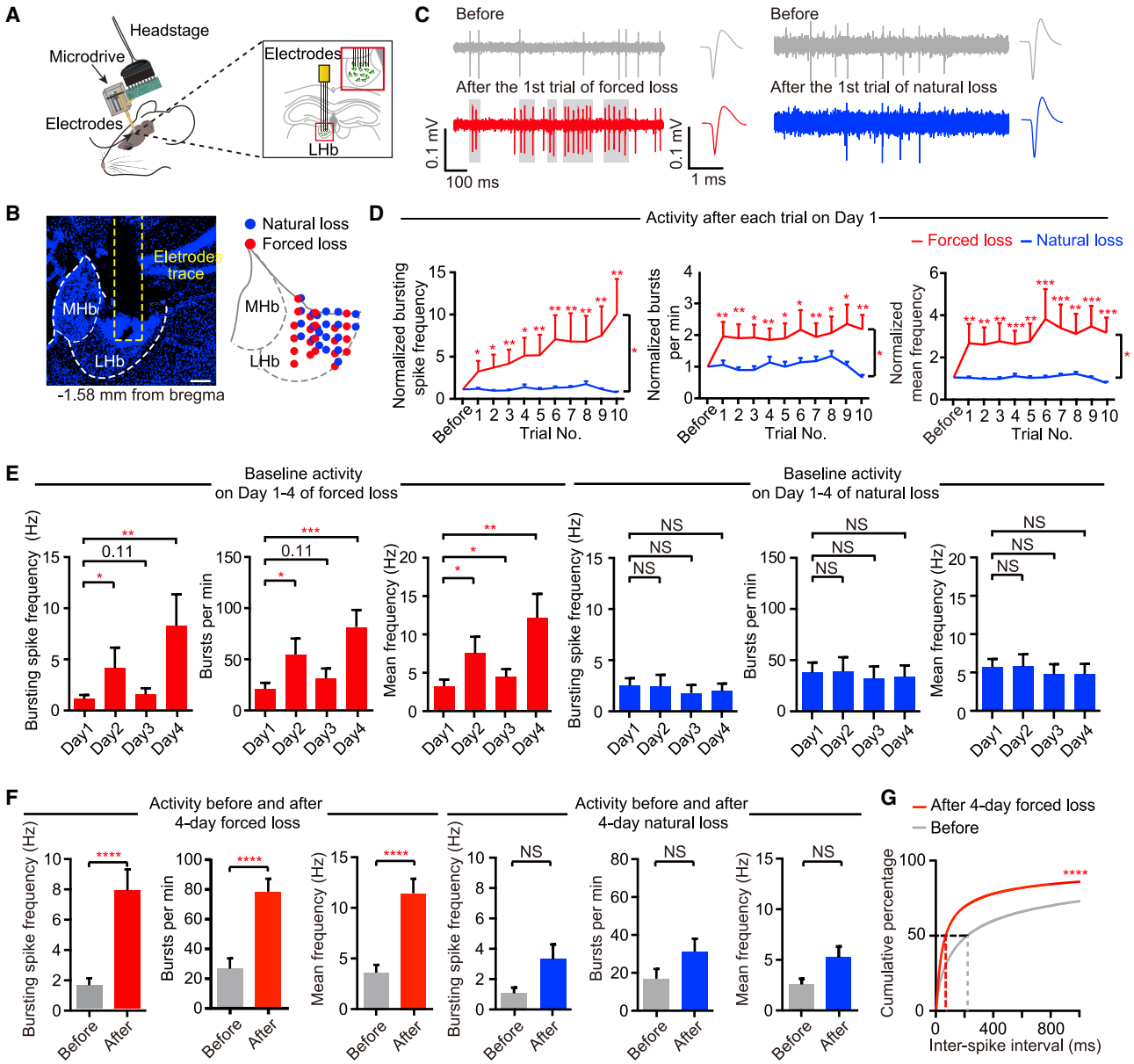

Figure 5. Forced loss induces LHb activation and burst firing

(A) Schematic of *in vivo* recording in LHb during forced or natural loss.

(B) An example recording site stained with Hoechst, with yellow dotted lines indicating the track of electrodes (left) and summary of recording sites in the LHb of natural loss (blue dots) and forced loss (red dots) mice (right). Scale bars, 100 μm.

(C) Example traces and averaged spike waveform of a recorded LHb neuron before (top) and after (bottom) the first trial of natural (right) or forced (left) loss. Bursts are identified by the inter-spike intervals (ISIs) method and indicated by gray shades.

(D) Normalized bursting spike frequency (left), normalized bursts per min (middle), and normalized mean frequency (right) of neurons across 10 trials on the 1st day of forced loss (red) and natural loss (blue).

(E) Baseline bursting spike frequency (left), bursts per min (middle), and mean frequency (right) of LHb neurons before the start of days 1–4 of forced loss (red) and natural loss (blue).

(F) Bursting spike frequency (left), bursts per min (middle), and mean frequency (right) of LHb neurons before and after 4 days of forced loss (red) and natural loss (blue).

(G) Cumulative distribution of ISIs of units before and after the 4-day forced loss. Dotted lines indicate the 50th percentile of ISI.

*p < 0.05; **p < 0.01; ***p < 0.001; ****p < 0.0001; ns, not significant. Data are represented as mean ± SEM. See also Figure S5.

Please cite this article in press as: Fan et al., Neural mechanism underlying depressive-like state associated with social status loss, Cell (2023), https://doi.org/10.1016/j.cell.2022.12.033

CellPress

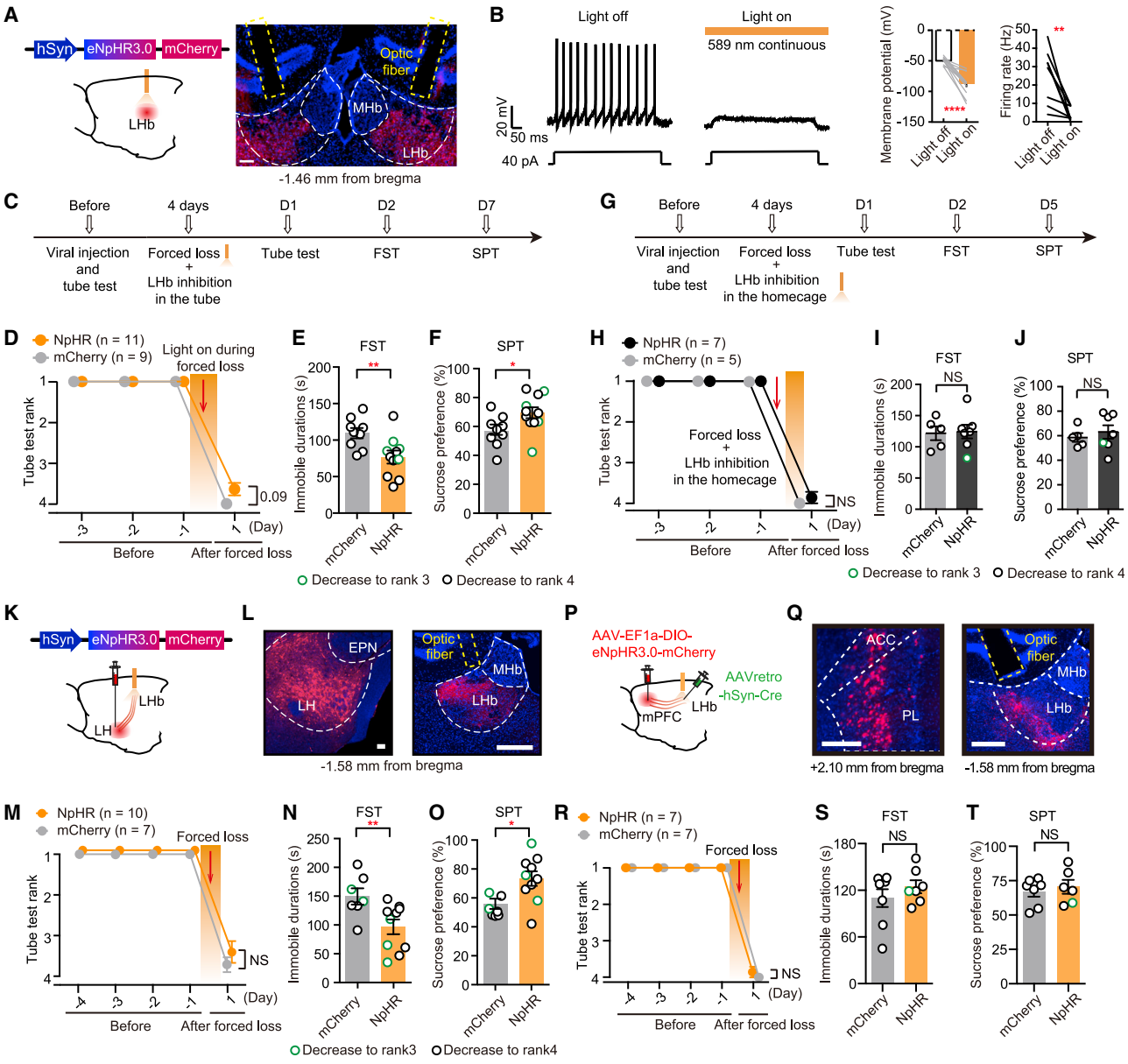

Figure 6. Inhibition of LHb or LH-LHb during forced loss prevents the induction of depressive-like behaviors

(A) Schematic illustrating the NpHR viral construct and viral injection site (left) and an example viral-expressing site (right). The location of optic fiber placement is indicated by the yellow dotted line. Red, NpHR; blue, Hoechst. Scale bars, 100 μm.

(B) Inhibitory effect of yellow light on eNpHR3.0-expressing LHb neurons. Left, sample traces of whole-cell patch-clamp recording in the LHb slices under current-clamp mode in light off and on conditions. Middle, the membrane potential of neurons during light off and light on. Right, the firing rate of neurons during light off and light on.

(C) Experimental paradigm for viral injection, optogenetic manipulation, and behavioral tests for (D–F).

(D) Tube test rank of mice expressing NpHR (orange) and mCherry (gray) in the LHb before and after forced loss with photostimulation. x axis is labeled by days before or after the 4-day forced loss procedure.

(E and F) Depressive-like behaviors of mCherry-expressing and NpHR-expressing groups. Mice decreasing to rank4 and rank3 are marked in black and green, respectively.

(G) Experimental paradigm for viral injection, optogenetic manipulation, and behavioral tests for (H–J).

(H) Daily tube test results of mice before and after the 4-day forced loss followed by LHb inhibition in the homecage. X axis is labeled by days before or after the 4-day forced loss procedure.

(I and J) Depressive-like behaviors of mice expressing mCherry and NpHR in LHb.

(K) Schematic illustrating the NpHR viral construct, viral injection site, and implantation site of the optic fiber for LH-LHb inhibition.

(legend continued on next page)

Please cite this article in press as: Fan et al., Neural mechanism underlying depressive-like state associated with social status loss, Cell (2023), https://doi.org/10.1016/j.cell.2022.12.033

procedure, the baseline activity of the LHb had a trend to keep climbing (Figure 5E). There was a significant increase after the 4-day forced loss in the bursting, tonic, and overall unit activities (Figures 5F and S5L). Because neural activity can potentially be influenced by behaviors of the reciprocal mouse,[42,48] we again included a natural loss control experiment in which rank1 mice competed against previously encountered, more dominant, inter-cage rank1 opponents. In these control mice, no significant increase in LHb burst firing or overall activity was observed (Figures 5D–5F, S5L, and S5N), suggesting that the increase of LHb bursts in mice experiencing forced loss was not simply due to pushes by the opponents. In addition, LHb units displayed clear differences in the cumulative frequency distribution of inter-spike intervals (ISIs) after the 4-day forced loss (Figure 5G), consistent with an increase in burst firing.

Inhibition of LHb or LH-LHb pathway during forced loss prevents induction of depressive-like behaviors

Investigating whether LHb activation is required for forced-loss-induced depressive-like behavior, we applied optogenetics to inhibit the LHb during the forced loss procedure (Figure 6). AAV viral vector was used to express the eNpHR3.0 (an enhanced variant of the inhibitory halorhodopsin),[51] together with mCherry, in LHb (Figures 6A and S6A), and whole-cell electrophysiology recording confirmed the inhibitory effect of eNpHR3.0 in LHb neurons (Figure 6B). Mice after surgery stably maintained their rank1 position (Figure S6B). We then switched on the yellow light right after two mice entered the tube and kept it on throughout the 10 × forced trials (Figure 6C). Photoinhibition did not prevent inner-cage rank decline induced by forced loss (Figure 6D), but it caused a significant reduction in depressive-like phenotypes in the FST (Figure 6E) and SPT (Figure 6F). As a control, inhibition of LHb neurons in the homecage using the same protocol after the daily forced loss did not reduce depressive-like behaviors (Figures 6G–6J).

We next tested the contribution of the LH-LHb pathway by expressing AAV-hSyn-eNpHR3.0-mCherry in the LH and implanting optic fiber above the LHb to inhibit the LH terminals in the LHb during the 4-day forced loss procedure (Figures 6K and 6L). With this manipulation, mice still experienced rank loss (Figure 6M) but were more resilient to depressive-like behaviors (Figures 6N and 6O). Such effect was not observed in optogenetic inhibition of the mPFC-LHb pathway (Figures 6P–6T). These results suggest that activation of the LH-LHb pathway during forced loss is necessary for the induction of a depressive-like state and that preventing it may fend off depressive state induced by loss of social status.

Activation of LHb shifts E/I balance in dmPFC and facilitates loss

Regarding the functional consequence of the depressive state in the competition itself, the social competition hypothesis of depression predicts that depressive mood should reduce social competitiveness.[2,15] To test this experimentally, we optogenetically activated the LHb, mimicking a depressive-like state,[32] and examined tube test competition. AAV-hSyn-ChrimsonR-tdTomato was injected into the LHb, above which an optic fiber was implanted (Figures 7A, 7B, and S7A). After the tube test rank was stable and ChrimsonR was fully expressed, the high-ranked mice were stimulated with red light during the tube test. Upon stimulation, these mice displayed much more retreat behaviors, leading to loss to their previous subordinate opponents (Figures 7C and S7B; Video S4). Stimulation of the LH-LHb, but not the mPFC-LHb pathway, caused similar losing effects in tube tests (Figures S7C–S7H). These results suggest that increased LHb activity during the depressive-like state may facilitate further loss in social competition.

We next investigated which neural substrate may mediate the effects of LHb activation on losing behavior. The dorsal mPFC (dmPFC) was found to play a critical role in controlling competitiveness, with its higher activity favoring winning.[40,52,53] Therefore, we examined the impact of LHb activation on dmPFC neural network activity. *In vivo* single-unit recording was conducted in the dmPFC when the LHb was optogenetically activated (Figure 7D). 168 well-isolated units were recorded from 5 mice and classified into 133 wide-spike, putative pyramidal (pPYR) neurons and 35 narrow-spike, putative interneurons (pIN)[54,55] (Figure S7I). Notably, during optogenetically induced LHb activation, a larger fraction (48.9%) of mPFC-pPYR neurons were inhibited (Figures 7E–7I and S7J), whereas a larger fraction (42.8%) of mPFC-pINs were excited (Figures 7F and S7J–S7M). There was a decrease in the overall pPYR activity (Figures 7F–7I and S7J). These results suggest that LHb activation can shift the E/I balance of mPFC neural activity toward more inhibition, which may account for the subordinate behaviors under the depressive state.

Antidepressant ketamine elevates social rank in dethroned mice

A second prediction from the social competition hypothesis of depression is that amelioration of a depressive-like state should

(L) An example of the viral injection site in the LH (left) and terminal site in the LHb (right). Red, NpHR; blue, Hoechst. Location of optic fiber placement is indicated by the yellow dotted line. Scale bars, 200 μm.
(M) Tube test rank of mice expressing NpHR (yellow) and mCherry (gray) before and after forced loss with photostimulation. x axis is labeled by days before or after the 4-day forced loss procedure.
(N and O) Depressive-like behaviors of mice expressing mCherry (gray) and NpHR (yellow) in the LH and optic fiber implanted in the LHb.
(P) Schematic illustrating the NpHR viral construct, viral injection site, and implantation site of the optic fiber for mPFC-LHb inhibition.
(Q) An example of viral injection site in the mPFC (left) and terminal site in the LHb (right). Red, NpHR; blue, Hoechst. Location of optic fiber placement is indicated by the yellow dotted line. Scale bars, 200 μm.
(R) Tube test rank of mice expressing NpHR (yellow) and mCherry (gray) before and after forced loss procedure with photostimulation. x axis is labeled by days before or after the 4-day forced loss procedure.
(S and T) Depressive-like behaviors of mice expressing mCherry (gray) and NpHR (yellow) in the mPFC and optic fiber implanted in the LHb.
*$p < 0.05$; **$p < 0.01$; ****$p < 0.0001$; ns, not significant. Data are represented as mean ± SEM. See also Figure S6.

Please cite this article in press as: Fan et al., Neural mechanism underlying depressive-like state associated with social status loss, Cell (2023), https://doi.org/10.1016/j.cell.2022.12.033

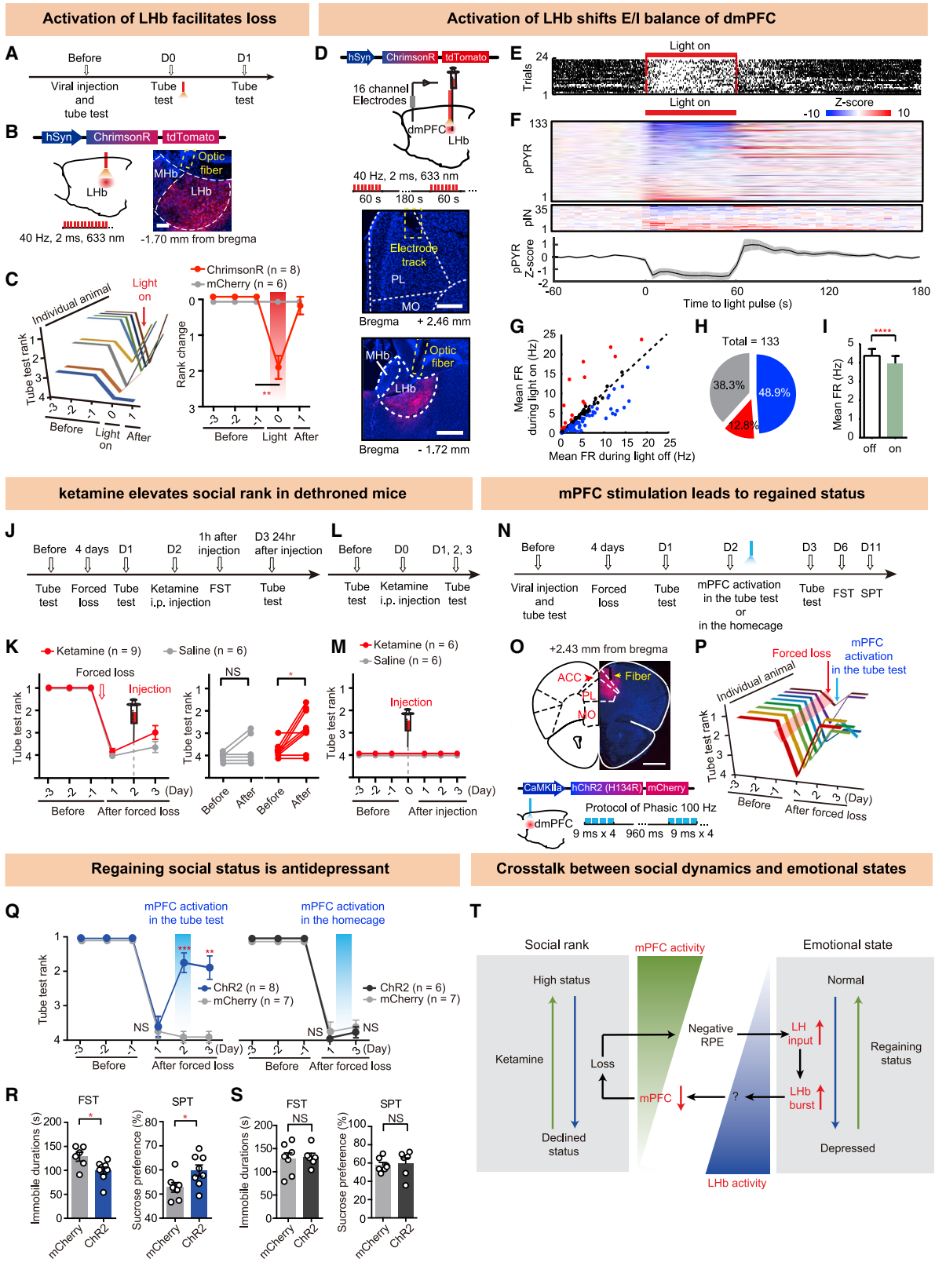

(legend on next page)

Please cite this article in press as: Fan et al., Neural mechanism underlying depressive-like state associated with social status loss, Cell (2023), https://doi.org/10.1016/j.cell.2022.12.033

change the behavioral pattern or coping strategy such that rank-declined animals become more willing to compete for their social positions. To test this, we injected mice with the rapid antidepressant ketamine after forced loss and on the following day tested their rank position (Figure 7J). Ketamine reduced depressive-like behaviors of forced loss mice within 1 h of injection (Figures 2J and 2K). Notably, 1 day after ketamine injection, a partial returning of the rank status was observed (Figure 7K). The rank-changed animals also showed increased pushes and decreased voluntary retreats in the tube test (Figure S7N). Interestingly, none of the normal rank4 mice showed elevation in rank after ketamine injection (Figures 7L and 7M), suggesting that ketamine's effect on rank elevation is specific to mice with recent experiences of forced loss.

Regaining social status after forced loss by activation of dmPFC is antidepressant

If a depressive-like state is induced by a loss of social status, could it be reversed by the regaining of the status? Since activation of the dmPFC induces instant winning and elevates social rank,[40,52,54,56] we tried optogenetically activating the dmPFC during the tube tests to restore the social status of rank-declined mice. AAV virus expressing CaMKII-hChR2 (H134R)-mCherry was injected into the dmPFC of rank1 mouse with optic fibers implanted 300 μm above the injection site (Figures 7N and 7O). These mice were subjected to forced loss and dropped to rank2, 3, or 4 (Figure 7P). We then induced repeated winning (10 times) by activating the dmPFC in tube tests (Figures 7O, S7O, and S7P). This resulted in returned rank in most of the stimulated mice (Figure 7P), in contrast to control mice expressing mCherry that stayed at the bottom rank after the same photostimulation protocol (Figure 7Q). Notably, mice regaining their dominant ranks showed reduced depressive-like phenotypes compared with the control group (Figure 7R). To make sure that this antidepressant effect was not simply due to stimulation of dmPFC neurons, we also tested a group of forced loss mice that received the same protocol of photostimulation in the homecage (Figure 7N). Their ranks remained at the bottom in the tube test (Figure 7Q) and depressive-like behaviors were not alleviated, compared with controls (Figure 7S), suggesting that this 4 min of dmPFC stimulation was not sufficient to cause antidepressant effects by itself.

DISCUSSION

Taken together, we propose a model whereby unpredicted-loss-triggered negative RPE activates the input from the LH to LHb and induces burst firing of LHb neurons, accounting for depressive-like behaviors induced by downward social mobility (Figure 7T). In particular, we identify a positive feedback mechanism that reinforces losing and depressive-like behaviors during status decline: the negative RPE signal activates LHb neurons (Figures 4 and 5D); LHb activation inhibits the dmPFC network activity, weakens the grit of mice during the confrontation, and leads to a higher chance of further loss (Figure 7); and to close the loop, the repetitive losing accumulatively further enhances the LHb baseline activities (Figure 5E), establishing the depression pathology. Importantly, however, this vicious cycle can be broken at each end of the feedback loop: at the one end, antidepressant treatment by ketamine increases the probability

Figure 7. Reciprocal interactions between mood and social rank

(A) Experimental paradigm for optogenetically activating LHb during tube tests.

(B) Left: schematic of the ChrimsonR viral construct. Right: an example LHb site showing viral expression and optic fiber implantation (outlined by yellow dotted line). Red, ChrimsonR; blue, Hoechst. Scale bars, 100 μm.

(C) Tube test rank of individual mice expressing ChrimsonR (left) and summary of tube test rank of all mice expressing ChrimsonR and mCherry (right) during light on. Light stimulation was delivered throughout the tube test at day 0.

(D) Schematic illustrating ChrimsonR viral construct, viral injection site in LHb (top), 16-channel electrodes in dmPFC (middle), and implantation sites of optic fiber in LHb (bottom). Red, ChrimsonR; blue, Hoechst. Scale bars, 200 μm.

(E) Raster plot of a representative unit aligned to the timestamp of light pulse.

(F) PSTH of the *Z* score of all neurons, including putative pyramidal neurons (pPYRs, top) and putative interneurons (pINs, middle), in ascending order of *Z* score during the 60-s light-on period. Average PSTH of the *Z* score of all pPYR units (bottom).

(G) Scatterplots of mean firing rate (FR) of pPYR units during light-off epoch against light-on epoch. Colored circles indicate units that show significant light-induced FR increase (red), decrease (blue), and no change (black).

(H) Pie graphs showing the percentage of pPYR units that have significantly higher (red), lower (blue), or unchanged (gray) FR during light stimulation.

(I) Mean FRs of pPYR units during light-off and light-on epochs.

(J–L) (J and L) Experimental paradigm for testing effects of ketamine on tube test ranks of recently dethroned (J) or stably subordinate (L) mice. (K) Tube test rank of mice injected with ketamine (red) or saline (gray) after forced loss. x axis is labeled by days before and after the 4-day forced loss procedure.

(M) Tube test rank of stable rank4 mice after injection of ketamine (red) or saline (gray).

(N) Experimental paradigm for restoring social status in forced loss mice and testing depressive-like behaviors.

(O) Schematic of viral construct, viral expression, optic fiber implantation (yellow arrowhead) in the dmPFC (top), and protocol of optogenetic stimulation (bottom). Red, ChR2; blue, Hoechst. Scale bars, 500 μm.

(P and Q) Tube test rank of mice expressing ChR2 in the dmPFC before and after forced loss and 10× photostimulated winning in the tube test (individual mice shown in P; summary shown in Q, left) or 10× dmPFC photostimulation in the homecage (Q, right).

(R and S) Depressive-like behaviors of mCherry- and ChR2- expressing mice after 10× dmPFC photostimulation in the tube test (R) or after dmPFC photostimulation in the homecage (S).

(T) Working model. Loss of competition to previous subordinate opponents triggers a negative social RPE, which instigates increased LHb bursting firing through the LH input to cause a depressive-like state. The increase in LHb bursts facilitates further loss, leading to reinforced subordination. This vicious cycle can be potentially hindered at both ends: regaining of social status can quickly ameliorate a depressive-like state, and mitigation of the depressive-like behaviors by antidepressants can lead to ascending status in newly dethroned mice. The question mark indicates an indirect connection.

*p < 0.05; **p < 0.01; ***p < 0.001; ****p < 0.0001; ns, not significant. Data are represented as mean ± SEM. See also Figure S7 and Video S4.

Please cite this article in press as: Fan et al., Neural mechanism underlying depressive-like state associated with social status loss, Cell (2023), https://doi.org/10.1016/j.cell.2022.12.033

of winning and the status of newly dethroned mice (Figure 7K); at the other end, regaining of social status by mPFC activation can quickly ameliorate depressive-like behaviors (Figure 7R). The discovery of such crosstalk provides a conceptual ground for potential behavioral intervention and treatment of depression caused by a major social-psychological factor.

Social descending paradigm as a mouse model of depression

Previously, social descending has been mostly studied in cichlid fish, where an intruder rival is introduced to challenge the dominant resident. The resident who fails to defend its territory and reproductive opportunities develops a series of changes along the neural-endocrine, reproductive, and stress axes,[12,13,57] as well as changes in behavioral patterns.[13,58] However, the limited manipulation tools in cichlid fish hindered further mechanistic studies. Here, we take the tube test as an opportunity to manipulate the social system in mice and create a social descending paradigm to study the behavioral and neurobiological changes during dynamic social reorganization. As a model for depression, the social descending paradigm meets the face, construct, and predictive validity to model human depression,[59–62] and it should provide a valuable tool for screening antidepressant drugs and exploring the etiological mechanism of depression, especially those involving social-mental factors.

Role of negative social reward prediction error

During social competition, humans or animals form a prediction of the competition outcome, based on the previous history of winning or losing against the conspecific.[63–68] Such prediction guides animals to adjust behaviors to either escalate the conflict and attack or to appease the conflict and be submissive.[2,14,69–71] For dominant animals, which have a wealth of winning experience, victory in competition becomes the default expectation.[68] Consistently, dominant animals are also more vulnerable to depression induced by chronic social defeat stress (CSDS, during which mice or rats are exposed to attacks by an extremely aggressive opponent for multiple days[61,72]) than their subordinate cagemates.[73]

The central role of LHb in encoding negative RPE was first illustrated in a classical reward conditioning experiment.[74] When the monkey did not receive the sound-conditioned juice reward, LHb neurons were activated. Here, we revealed a negative RPE in a social context—the unexpected loss to an ex-subordinate cagemate. When activated, the LHb can transmit a negative motivational signal by inhibiting the downstream aminergic reward circuitry.[75] While acute activation of the LHb can induce aversiveness,[32] repeated activation of the LHb will eventually lead to a depressive-like state, manifested as behavioral despair and anhedonia.[16,76]

The neural circuitry underlying depression-reinforced subordination

Our results provide direct experimental evidence for the social competition hypothesis of depression, demonstrating that mice in the depressive-like state, induced by LHb activation, tend to lose in competition. Such subordinate behavioral patterns will prevent attempts to make "come-back" fights, protecting animals from further confrontations and potential injuries.[2] In an effort to explore the neural mechanisms underlying this depression-reinforced subordination, we found that LHb activation inhibits the dmPFC global network activity (Figures 7E–7I and S7I–S7M). Although the LHb does not directly project to the mPFC, its downstream target, the ventral tegmental area dopamine (VTA-DA) neurons innervate the mPFC.[77] Given that the LHb inhibits VTA-DA neurons[26] and that activation of VTA-DA neurons increases c-Fos expression[78] and enhances signal-to-noise ratio[79] in the mPFC, VTA-DA may be a potential node through which LHb suppresses mPFC ensemble activity to reinforce a "loser" state.

Antidepressant and social hierarchy status

Chronic treatment with classical antidepressants has been shown to increase aggression and elevate status in the social hierarchy.[80] The antidepressants used in these studies were all slow-acting serotonin/norepinephrine reuptake inhibitors (SNRI) or the selective serotonin reuptake inhibitors (SSRI) types, which take at least 1 to 2 weeks to show antidepressant effects and require repeated treatments. Such slow action makes it difficult to distinguish the direct versus indirect effects of these drugs on social status. In this study, we used a rapid-acting antidepressant, ketamine, which has a rapid action onset and high efficacy.[43,81–83] Mechanistically, ketamine rapidly suppresses LHb burst firing to elicit antidepressant effects.[32,49] We found that a single application of ketamine ameliorated social-descending-induced anhedonia- and despair-like phenotypes in 1 h (Figures 2J and 2K). Without bolstering aggression,[84] ketamine partially restored social status, accompanied by more effortful behaviors, within 24 h of administration (Figures 7K and S7N). By contrast, ketamine failed to induce more effortful behaviors or increase status in natural subordinate mice (normal rank4) (Figure 7M). This distinction suggests that the crosstalk between LHb hyperactivation and social competitiveness may be an acquired connection during the social status decline. In descending mice, ketamine quenches the LHb burst firing and releases the social competitiveness from the inhibitory control of LHb activities; in mice with an established low rank, LHb activity is conditioned at a low level, and this crosstalk is not initiated, therefore ketamine does not have any impact.

Limitations of the study

One limitation of the "forced loss" paradigm as an animal model for depression is that it can only be applied to mice at a relatively more dominant position. Since low-rank mice are more resilient to stress[73] and are used to loss, forced loss cannot produce negative RPE and induce depressive-like behaviors in these subordinate mice. Another limitation of the study is that only male mice were used, and it needs to be tested in the future whether similar neural and behavioral effects are shared by females[85]. In terms of intervention of the social-status-loss-induced depressive state, we applied optogenetic activation of the dmPFC to induce repeated winning (Figures 7P–7S). While effective, this methodology is invasive and artificial. A more natural, non-invasive behavioral strategy to reverse social-status-loss-induced depressive-like behaviors should be explored in the future.

STAR★METHODS

Detailed methods are provided in the online version of this paper and include the following:

- KEY RESOURCES TABLE
- RESOURCE AVAILABILITY
  - Lead contact
  - Materials availability
  - Data and code availability
- EXPERIMENTAL MODEL AND SUBJECT DETAILS
- METHOD DETAILS
  - Behavioral assays
  - Surgery and viral injection
  - Optogenetic manipulation in tube test and forced loss
  - Systemic ketamine administration
  - Fiber photometry recording
  - Electrophysiological Recordings
  - c-Fos Immunohistochemistry staining and counting
- QUANTIFICATION AND STATISTICAL ANALYSIS

SUPPLEMENTAL INFORMATION

Supplemental information can be found online at https://doi.org/10.1016/j.cell.2022.12.033.

ACKNOWLEDGMENTS

We thank H. Kessels for stimulating discussions and critical comments on the manuscript; K. Deisseroth and Z. Qiu for AAV-ChR2 constructs; H. Li, X. Xiang, and K. Sang for advice on single electrodes production and data analysis of *in vivo* recording; T. Zhou, Z. Ni, H. Liang, P. Wu and colleagues from Hu lab for assistance in experiments. This work was supported by the STI2030-Major Projects (2021ZD0203000 (2021ZD0203001)) , the National Natural Science Foundation of China (32130042 and 31830032), the Key-Area Research and Development Program of Guangdong Province (2018B030334001 and 2018B030331001), the National Key Research and Development Program of China (2016YFA0501000), the 111 Project (B13026), the Fountain-Valley Life Sciences Fund of University of Chinese Academy of Sciences Education Foundation and the CAMS Innovation Fund for Medical Sciences (2019-I2M-5-057), the Key R&D Program of Zhejiang Province (2020C03009), the Starry Night Science Fund of Zhejiang University Shanghai Institute for Advanced Study (SN-ZJU-SIAS-002), the Project for Hangzhou Medical Disciplines of Excellence, and Key Project for Hangzhou Medical Disciplines to H.H., and by the Zhejiang Provincial Natural Science Foundation of China (LY23C090003), and the project was funded by the China Postdoctoral Science Foundation (2022M722775) to Z.F.

AUTHOR CONTRIBUTIONS

Z.F., J.C., Y.L., H.Z., and Y.X. conducted the optogenetic manipulation, the behavioral pharmacology experiments, and the related behavioral analysis. Z.F., J.C., and D.Z. performed the *in vivo* electrophysiology recordings and fiber photometry. J.W. performed the *in vitro* electrophysiology recordings. H.H., Z.F., and Q.-J.L. designed the study. H.H. supervised the project and wrote the manuscript with the assistance of Z.F. and Q.-J.L.

DECLARATION OF INTERESTS

H.H. is a member of the advisory board of *Cell*.

INCLUSION AND DIVERSITY

One or more of the authors of this paper self-identifies as a member of the LGBTQIA+ community.

Received: January 18, 2022
Revised: October 13, 2022
Accepted: December 20, 2022
Published: January 23, 2023

REFERENCES

1. Brown, G.W., and Harris, T. (1978). The Social Origins of Depression (Tavistock Press).
2. Price, J., Sloman, L., Gardner, R., Jr., Gilbert, P., and Rohde, P. (1994). The social competition hypothesis of depression. Br. J. Psychiatry *164*, 309–315. https://doi.org/10.1192/bjp.164.3.309.
3. Sapolsky, R.M. (2004). Social status and health in humans and other animals. Annu. Rev. Anthropol. *33*, 393–418. https://doi.org/10.1146/annurev.anthro.33.070203.144000.
4. Tiffin, P.A., Pearce, M.S., and Parker, L. (2005). Social mobility over the lifecourse and self reported mental health at age 50: prospective cohort study. J. Epidemiol. Community Health *59*, 870–872. https://doi.org/10.1136/jech.2005.035246.
5. Nicklett, E.J., and Burgard, S.A. (2009). Downward social mobility and major depressive episodes among Latino and Asian-American immigrants to the United States. Am. J. Epidemiol. *170*, 793–801. https://doi.org/10.1093/aje/kwp192.
6. Brewer, G., and Olive, N. (2014). Depression in men and women: relative rank, interpersonal dependency, and risk-taking. Evol. Behav. Sci. *8*, 142–147. https://doi.org/10.1037/h0097761.
7. COVID-19 Mental Disorders Collaborators (2021). Global prevalence and burden of depressive and anxiety disorders in 204 countries and territories in 2020 due to the COVID-19 pandemic. Lancet *398*, 1700–1712. https://doi.org/10.1016/S0140-6736(21)02143-7.
8. Goodall, J. (1986). Chimpanzees of Gombe: Patterns of Behavior (Harvard University Press).
9. Brain, C.K. (1965). Observations on the behaviour of vervet monkeys Cercopithecus aethiops. Zool. Afr. *1*, 13–27. https://doi.org/10.1080/00445096.1965.11447296.
10. Schjelderup-Ebbe, T. (1922). Beitrage zur Sozialpsycholgie des Haushuhns. Z. Psychol. *88*, 225–252. https://psycnet.apa.org/record/1926-07009-001.
11. MacLean, P.D. (1990). The Triune Brain in Evolution (Plenum Press).
12. Francis, R.C., Soma, K., and Fernald, R.D. (1993). Social regulation of the brain-pituitary-gonadal axis. Proc. Natl. Acad. Sci. USA *90*, 7794–7798. https://doi.org/10.1073/pnas.90.16.7794.
13. Maruska, K.P., Becker, L., Neboori, A., and Fernald, R.D. (2013). Social descent with territory loss causes rapid behavioral, endocrine and transcriptional changes in the brain. J. Exp. Biol. *216*, 3656–3666. https://doi.org/10.1242/jeb.088617.
14. Nakajo, H., Tsuboi, T., and Okamoto, H. (2020). The behavioral paradigm to induce repeated social defeats in zebrafish. Neurosci. Res. *161*, 24–32. https://doi.org/10.1016/j.neures.2019.11.004.
15. Price, J. (1967). The dominance hierarchy and the evolution of mental illness. Lancet *290*, 243–246. https://doi.org/10.1016/S0140-6736(67)92306-9.
16. Proulx, C.D., Hikosaka, O., and Malinow, R. (2014). Reward processing by the lateral habenula in normal and depressive behaviors. Nat. Neurosci. *17*, 1146–1152. https://doi.org/10.1038/nn.3779.
17. Yang, Y., Wang, H., Hu, J., and Hu, H. (2018). Lateral habenula in the pathophysiology of depression. Curr. Opin. Neurobiol. *48*, 90–96. https://doi.org/10.1016/j.conb.2017.10.024.

18. Wirtshafter, D., Asin, K.E., and Pitzer, M.R. (1994). Dopamine agonists and stress produce different patterns of Fos-like immunoreactivity in the lateral habenula. Brain Res. *633*, 21–26. https://doi.org/10.1016/0006-8993(94)91517-2.

19. Huang, L., Xi, Y., Peng, Y., Yang, Y., Huang, X., Fu, Y., Tao, Q., Xiao, J., Yuan, T., An, K., et al. (2019). A visual circuit related to habenula underlies the antidepressive effects of light therapy. Neuron *102*, 128–142.e8. https://doi.org/10.1016/j.neuron.2019.01.037.

20. Wang, D., Li, Y., Feng, Q., Guo, Q., Zhou, J., and Luo, M. (2017). Learning shapes the aversion and reward responses of lateral habenula neurons. eLife *6*, e23045. https://doi.org/10.7554/eLife.23045.

21. Flanigan, M.E., Aleyasin, H., Li, L., Burnett, C.J., Chan, K.L., LeClair, K.B., Lucas, E.K., Matikainen-Ankney, B., Durand-de Cuttoli, R., Takahashi, A., et al. (2020). Orexin signaling in GABAergic lateral habenula neurons modulates aggressive behavior in male mice. Nat. Neurosci. *23*, 638–650. https://doi.org/10.1038/s41593-020-0617-7.

22. Amo, R., Fredes, F., Kinoshita, M., Aoki, R., Aizawa, H., Agetsuma, M., Aoki, T., Shiraki, T., Kakinuma, H., Matsuda, M., et al. (2014). The habenulo-raphe serotonergic circuit encodes an aversive expectation value essential for adaptive active avoidance of danger. Neuron *84*, 1034–1048. https://doi.org/10.1016/j.neuron.2014.10.035.

23. Golden, S.A., Heshmati, M., Flanigan, M., Christoffel, D.J., Guise, K., Pfau, M.L., Aleyasin, H., Menard, C., Zhang, H., Hodes, G.E., et al. (2016). Basal forebrain projections to the lateral habenula modulate aggression reward. Nature *534*, 688–692. https://doi.org/10.1038/nature18601.

24. Flanigan, M., Aleyasin, H., Takahashi, A., Golden, S.A., and Russo, S.J. (2017). An emerging role for the lateral habenula in aggressive behavior. Pharmacol. Biochem. Behav. *162*, 79–86. https://doi.org/10.1016/j.pbb.2017.05.003.

25. Ferraro, G., Montalbano, M.E., Sardo, P., and La Grutta, V. (1996). Lateral habenular influence on dorsal raphe neurons. Brain Res. Bull. *41*, 47–52. https://doi.org/10.1016/0361-9230(96)00170-0.

26. Gao, D.M., Jeaugey, L., Pollak, P., and Benabid, A.L. (1990). Intensity-dependent nociceptive responses from presumed dopaminergic neurons of the substantia nigra, pars compacta in the rat and their modification by lateral habenula inputs. Brain Res. *529*, 315–319. https://doi.org/10.1016/0006-8993(90)90843-z.

27. Zhou, L., Liu, M.Z., Li, Q., Deng, J., Mu, D., and Sun, Y.G. (2017). Organization of functional long-range circuits controlling the activity of serotonergic neurons in the dorsal raphe nucleus. Cell Rep. *18*, 3018–3032. https://doi.org/10.1016/j.celrep.2017.02.077.

28. Caldecott-Hazard, S., Mazziotta, J., and Phelps, M. (1988). Cerebral correlates of depressed behavior in rats, visualized using 14C-2-deoxyglucose autoradiography. J. Neurosci. *8*, 1951–1961. https://doi.org/10.1523/JNEUROSCI.08-06-01951.1988.

29. Morris, J.S., Smith, K.A., Cowen, P.J., Friston, K.J., and Dolan, R.J. (1999). Covariation of activity in habenula and dorsal raphe nuclei following tryptophan depletion. NeuroImage *10*, 163–172. https://doi.org/10.1006/nimg.1999.0455.

30. Mirrione, M.M., Schulz, D., Lapidus, K.A., Zhang, S., Goodman, W., and Henn, F.A. (2014). Increased metabolic activity in the septum and habenula during stress is linked to subsequent expression of learned helplessness behavior. Front. Hum. Neurosci. *8*, 29. https://doi.org/10.3389/fnhum.2014.00029.

31. Andalman, A.S., Burns, V.M., Lovett-Barron, M., Broxton, M., Poole, B., Yang, S.J., Grosenick, L., Lerner, T.N., Chen, R., Benster, T., et al. (2019). Neuronal dynamics regulating brain and behavioral state transitions. Cell *177*, 970–985.e20. https://doi.org/10.1016/j.cell.2019.02.037.

32. Yang, Y., Cui, Y., Sang, K., Dong, Y., Ni, Z., Ma, S., and Hu, H. (2018). Ketamine blocks bursting in the lateral habenula to rapidly relieve depression. Nature *554*, 317–322. https://doi.org/10.1038/nature25509.

33. Cerniauskas, I., Winterer, J., de Jong, J.W., Lukacsovich, D., Yang, H., Khan, F., Peck, J.R., Obayashi, S.K., Lilascharoen, V., Lim, B.K., et al. (2019). Chronic stress induces activity, synaptic, and transcriptional remodeling of the lateral habenula associated with deficits in motivated behaviors. Neuron *104*, 899–915.e8. https://doi.org/10.1016/j.neuron.2019.09.005.

34. Lindzey, G., Winston, H., and Manosevitz, M. (1961). Social dominance in inbred mouse strains. Nature *191*, 474–476. https://doi.org/10.1038/191474a0.

35. Wang, F., Kessels, H.W., and Hu, H. (2014). The mouse that roared: neural mechanisms of social hierarchy. Trends Neurosci. *37*, 674–682. https://doi.org/10.1016/j.tins.2014.07.005.

36. Wang, F., Zhu, J., Zhu, H., Zhang, Q., Lin, Z., and Hu, H. (2011). Bidirectional control of social hierarchy by synaptic efficacy in medial prefrontal cortex. Science *334*, 693–697. https://doi.org/10.1126/science.1209951.

37. Fan, Z., Zhu, H., Zhou, T., Wang, S., Wu, Y., and Hu, H. (2019). Using the tube test to measure social hierarchy in mice. Nat. Protoc. *14*, 819–831. https://doi.org/10.1038/s41596-018-0116-4.

38. van den Berg, W.E., Lamballais, S., and Kushner, S.A. (2015). Sex-specific mechanism of social hierarchy in mice. Neuropsychopharmacology *40*, 1364–1372. https://doi.org/10.1038/npp.2014.319.

39. Bicks, L.K., Peng, M., Taub, A., Akbarian, S., and Morishita, H. (2021). An adolescent sensitive period for social dominance hierarchy plasticity is regulated by cortical plasticity modulators in mice. Front. Neural Circuits *15*, 676308. https://doi.org/10.3389/fncir.2021.676308.

40. Zhou, T., Zhu, H., Fan, Z., Wang, F., Chen, Y., Liang, H., Yang, Z., Zhang, L., Lin, L., Zhan, Y., et al. (2017). History of winning remodels thalamo-PFC circuit to reinforce social dominance. Science *357*, 162–168. https://doi.org/10.1126/science.aak9726.

41. Saxena, K., Webster, J., Hallas-Potts, A., Mackenzie, R., Spooner, P.A., Thomson, D., Kind, P., Chattarji, S., and Morris, R.G.M. (2018). Experiential contributions to social dominance in a rat model of fragile-X syndrome. Proc. Biol. Sci. *285*, 20180294. https://doi.org/10.1098/rspb.2018.0294.

42. Sterley, T.L., Baimoukhametova, D., Füzesi, T., Zurek, A.A., Daviu, N., Rasiah, N.P., Rosenegger, D., and Bains, J.S. (2018). Social transmission and buffering of synaptic changes after stress. Nat. Neurosci. *21*, 393–403. https://doi.org/10.1038/s41593-017-0044-6.

43. Berman, R.M., Cappiello, A., Anand, A., Oren, D.A., Heninger, G.R., Charney, D.S., and Krystal, J.H. (2000). Antidepressant effects of ketamine in depressed patients. Biol. Psychiatry *47*, 351–354. https://doi.org/10.1016/s0006-3223(99)00230-9.

44. Cunningham, C.L., Gremel, C.M., and Groblewski, P.A. (2006). Drug-induced conditioned place preference and aversion in mice. Nat. Protoc. *1*, 1662–1670. https://doi.org/10.1038/nprot.2006.279.

45. Morgan, J.I., Cohen, D.R., Hempstead, J.L., and Curran, T. (1987). Mapping patterns of c-fos expression in the central nervous system after seizure. Science *237*, 192–197. https://doi.org/10.1126/science.3037702.

46. Farivar, R., Zangenehpour, S., and Chaudhuri, A. (2004). Cellular-resolution activity mapping of the brain using immediate-early gene expression. Front. Biosci. *9*, 104–109.

47. Xiu, J., Zhang, Q., Zhou, T., Zhou, T.T., Chen, Y., and Hu, H. (2014). Visualizing an emotional valence map in the limbic forebrain by TAI-FISH. Nat. Neurosci. *17*, 1552–1559. https://doi.org/10.1038/nn.3813.

48. Kingsbury, L., Huang, S., Wang, J., Gu, K., Golshani, P., Wu, Y.E., and Hong, W. (2019). Correlated neural activity and encoding of behavior across brains of socially interacting animals. Cell *178*, 429–446.e16. https://doi.org/10.1016/j.cell.2019.05.022.

49. Cui, Y., Yang, Y., Ni, Z., Dong, Y., Cai, G., Foncelle, A., Ma, S., Sang, K., Tang, S., Li, Y., et al. (2018). Astroglial Kir4.1 in the lateral habenula drives neuronal bursts in depression. Nature *554*, 323–327. https://doi.org/10.1038/nature25752.

50. Lecca, S., Trusel, M., and Mameli, M. (2017). Footshock-induced plasticity of GABAB signalling in the lateral habenula requires dopamine and glucocorticoid receptors. Synapse *71*. e21948. https://doi.org/10.1002/syn.21948.

51. Gradinaru, V., Thompson, K.R., and Deisseroth, K. (2008). eNpHR: a Natronomonas halorhodopsin enhanced for optogenetic applications. Brain Cell Biol. *36*, 129–139. https://doi.org/10.1007/s11068-008-9027-6.

52. Padilla-Coreano, N., Batra, K., Patarino, M., Chen, Z., Rock, R.R., Zhang, R., Hausmann, S.B., Weddington, J.C., Patel, R., Zhang, Y.E., et al. (2022). Cortical ensembles orchestrate social competition through hypothalamic outputs. Nature *603*, 667–671. https://doi.org/10.1038/s41586-022-04507-5.

53. Zhu, H., and Hu, H.L. (2018). Brain's neural switch for social dominance in animals. Sci. China Life Sci. *61*, 113–114. https://doi.org/10.1007/s11427-017-9181-1.

54. Zhang, C., Zhu, H., Ni, Z., Xin, Q., Zhou, T., Wu, R., Gao, G., Gao, Z., Ma, H., Li, H., et al. (2022). Dynamics of a disinhibitory prefrontal microcircuit in controlling social competition. Neuron *110*, 516–531.e6. https://doi.org/10.1016/j.neuron.2021.10.034.

55. Kim, H., Ährlund-Richter, S., Wang, X., Deisseroth, K., and Carlén, M. (2016). Prefrontal parvalbumin neurons in control of attention. Cell *164*, 208–218. https://doi.org/10.1016/j.cell.2015.11.038.

56. Li, S.W., Zeliger, O., Strahs, L., Báez-Mendoza, R., Johnson, L.M., McDonald Wojciechowski, A., and Williams, Z.M. (2022). Frontal neurons driving competitive behaviour and ecology of social groups. Nature *603*, 661–666. https://doi.org/10.1038/s41586-021-04000-5.

57. White, S.A., Nguyen, T., and Fernald, R.D. (2002). Social regulation of gonadotropin-releasing hormone. J. Exp. Biol. *205*, 2567–2581. https://doi.org/10.1242/jeb.205.17.2567.

58. Almeida, O., Félix, A.S., Oliveira, G.A., Lopes, J.S., and Oliveira, R.F. (2019). Fighting assessment triggers rapid changes in activity of the brain social decision-making network of cichlid fish. Front. Behav. Neurosci. *13*, 229. https://doi.org/10.3389/fnbeh.2019.00229.

59. McKinney, W.T., Jr., and Bunney, W.E., Jr. (1969). Animal model of depression. I. Review of evidence: implications for research. Arch. Gen. Psychiatry *21*, 240–248. https://doi.org/10.1001/archpsyc.1969.01740200112015.

60. Willner, P. (1984). The validity of animal models of depression. Psychopharmacol. (Berl.) *83*, 1–16. https://doi.org/10.1007/BF00427414.

61. Berton, O., McClung, C.A., Dileone, R.J., Krishnan, V., Renthal, W., Russo, S.J., Graham, D., Tsankova, N.M., Bolanos, C.A., Rios, M., et al. (2006). Essential role of BDNF in the mesolimbic dopamine pathway in social defeat stress. Science *311*, 864–868. https://doi.org/10.1126/science.1120972.

62. Nestler, E.J., and Hyman, S.E. (2010). Animal models of neuropsychiatric disorders. Nat. Neurosci. *13*, 1161–1169. https://doi.org/10.1038/nn.2647.

63. Ligneul, R., Obeso, I., Ruff, C.C., and Dreher, J.C. (2016). Dynamical representation of dominance relationships in the human rostromedial prefrontal cortex. Curr. Biol. *26*, 3107–3115. https://doi.org/10.1016/j.cub.2016.09.015.

64. Qu, C., Ligneul, R., Van der Henst, J.B., and Dreher, J.C. (2017). An integrative interdisciplinary perspective on social dominance hierarchies. Trends Cogn. Sci. *21*, 893–908. https://doi.org/10.1016/j.tics.2017.08.004.

65. Hsu, Y.Y., Earley, R.L., and Wolf, L.L. (2006). Modulation of aggressive behaviour by fighting experience: mechanisms and contest outcomes. Biol. Rev. Camb. Philos. Soc. *81*, 33–74. https://doi.org/10.1017/S146479310500686X.

66. Trannoy, S., and Kravitz, E.A. (2017). Strategy changes in subsequent fights as consequences of winning and losing in fruit fly fights. Fly *11*, 129–138. https://doi.org/10.1080/19336934.2016.1259041.

67. Dwortz, M.F., Curley, J.P., Tye, K.M., and Padilla-Coreano, N. (2022). Neural systems that facilitate the representation of social rank. Philos. Trans. R. Soc. Lond. B Biol. Sci. *377*, 20200444. https://doi.org/10.1098/rstb.2020.0444.

68. Wei, D., Talwar, V., and Lin, D. (2021). Neural circuits of social behaviors: innate yet flexible. Neuron *109*, 1600–1620. https://doi.org/10.1016/j.neuron.2021.02.012.

69. Allan, S., and Gilbert, P. (1997). Submissive behaviour and psychopathology. Br. J. Clin. Psychol. *36*, 467–488. https://doi.org/10.1111/j.2044-8260.1997.tb01255.x.

70. Torigoe, M., Islam, T., Kakinuma, H., Fung, C.C.A., Isomura, T., Shimazaki, H., Aoki, T., Fukai, T., and Okamoto, H. (2021). Zebrafish capable of generating future state prediction error show improved active avoidance behavior in virtual reality. Nat. Commun. *12*, 5712. https://doi.org/10.1038/s41467-021-26010-7.

71. Chou, M.Y., Amo, R., Kinoshita, M., Cherng, B.W., Shimazaki, H., Agetsuma, M., Shiraki, T., Aoki, T., Takahoko, M., Yamazaki, M., et al. (2016). Social conflict resolution regulated by two dorsal habenular subregions in zebrafish. Science *352*, 87–90. https://doi.org/10.1126/science.aac9508.

72. Kudryavtseva, N.N., Bakshtanovskaya, I.V., and Koryakina, L.A. (1991). Social model of depression in mice of C57BL/6J strain. Pharmacol. Biochem. Behav. *38*, 315–320. https://doi.org/10.1016/0091-3057(91)90284-9.

73. Larrieu, T., Cherix, A., Duque, A., Rodrigues, J., Lei, H., Gruetter, R., and Sandi, C. (2017). Hierarchical status predicts behavioral vulnerability and nucleus accumbens metabolic profile following chronic social defeat stress. Curr. Biol. *27*, 2202–2210.e4. https://doi.org/10.1016/j.cub.2017.06.027.

74. Matsumoto, M., and Hikosaka, O. (2007). Lateral habenula as a source of negative reward signals in dopamine neurons. Nature *447*, 1111–1115. https://doi.org/10.1038/nature05860.

75. Hikosaka, O. (2010). The habenula: from stress evasion to value-based decision-making. Nat. Rev. Neurosci. *11*, 503–513. https://doi.org/10.1038/nrn2866.

76. Hu, H., Cui, Y., and Yang, Y. (2020). Circuits and functions of the lateral habenula in health and in disease. Nat. Rev. Neurosci. *21*, 277–295. https://doi.org/10.1038/s41583-020-0292-4.

77. Lammel, S., Lim, B.K., Ran, C., Huang, K.W., Betley, M.J., Tye, K.M., Deisseroth, K., and Malenka, R.C. (2012). Input-specific control of reward and aversion in the ventral tegmental area. Nature *491*, 212–217. https://doi.org/10.1038/nature11527.

78. Gunaydin, L.A., Grosenick, L., Finkelstein, J.C., Kauvar, I.V., Fenno, L.E., Adhikari, A., Lammel, S., Mirzabekov, J.J., Airan, R.D., Zalocusky, K.A., et al. (2014). Natural neural projection dynamics underlying social behavior. Cell *157*, 1535–1551. https://doi.org/10.1016/j.cell.2014.05.017.

79. Vander Weele, C.M., Siciliano, C.A., Matthews, G.A., Namburi, P., Izadmehr, E.M., Espinel, I.C., Nieh, E.H., Schut, E.H.S., Padilla-Coreano, N., Burgos-Robles, A., et al. (2018). Dopamine enhances signal-to-noise ratio in cortical-brainstem encoding of aversive stimuli. Nature *563*, 397–401. https://doi.org/10.1038/s41586-018-0682-1.

80. Mitchell, P.J. (2005). Antidepressant treatment and rodent aggressive behaviour. Eur. J. Pharmacol. *526*, 147–162. https://doi.org/10.1016/j.ejphar.2005.09.029.

81. Murrough, J.W., Iosifescu, D.V., Chang, L.C., Al Jurdi, R.K., Green, C.E., Perez, A.M., Iqbal, S., Pillemer, S., Foulkes, A., Shah, A., et al. (2013). Antidepressant efficacy of ketamine in treatment-resistant major depression: a two-site randomized controlled trial. Am. J. Psychiatry *170*, 1134–1142. https://doi.org/10.1176/appi.ajp.2013.13030392.

82. Li, N., Lee, B., Liu, R.J., Banasr, M., Dwyer, J.M., Iwata, M., Li, X.Y., Aghajanian, G., and Duman, R.S. (2010). mTOR-dependent synapse formation underlies the rapid antidepressant effects of NMDA antagonists. Science *329*, 959–964. https://doi.org/10.1126/science.1190287.

83. Krystal, J.H., Abdallah, C.G., Sanacora, G., Charney, D.S., and Duman, R.S. (2019). Ketamine: A paradigm shift for depression research and

treatment. Neuron *101*, 774–778. https://doi.org/10.1016/j.neuron.2019.02.005.

84. Shin, S.Y., Baek, N.J., Han, S.H., and Min, S.S. (2019). Chronic administration of ketamine ameliorates the anxiety- and aggressive-like behavior in adolescent mice induced by neonatal maternal separation. Korean J. Physiol. Pharmacol. *23*, 81–87. https://doi.org/10.4196/kjpp.2019.23.1.81.

85. Xiao, W., Jiao, Z.-L., Senol, E., Yao, J., Zhao, M., Zhao, Z.-D., Chen, X., Cao, P., Fu, Y., Gao, Z., et al. (2022). Neural circuit control of innate behaviors. Sci China Life Sci *65*, 466–499. https://doi.org/10.1007/s11427-021-2043-2.

86. Friard, O., and Gamba, M. (2016). BORIS: a free, versatile open-source event-logging software for video/audio coding and live observations. Methods Ecol. Evol. *7*, 1325–1330. https://doi.org/10.1111/2041-210X.12584.

87. Yamaguchi, T., Wei, D., Song, S.C., Lim, B., Tritsch, N.X., and Lin, D. (2020). Posterior amygdala regulates sexual and aggressive behaviors in male mice. Nat. Neurosci. *23*, 1111–1124. https://doi.org/10.1038/s41593-020-0675-x.

88. Powell, T.R., Fernandes, C., and Schalkwyk, L.C. (2012). Depression-related behavioral tests. Curr. Protoc. Mouse Biol. *2*, 119–127. https://doi.org/10.1002/9780470942390.mo110176.

89. Slattery, D.A., and Cryan, J.F. (2012). Using the rat forced swim test to assess antidepressant-like activity in rodents. Nat. Protoc. *7*, 1009–1014. https://doi.org/10.1038/nprot.2012.044.

90. Li, Y., Zhong, W., Wang, D., Feng, Q., Liu, Z., Zhou, J., Jia, C., Hu, F., Zeng, J., Guo, Q., et al. (2016). Serotonin neurons in the dorsal raphe nucleus encode reward signals. Nat. Commun. *7*, 10503. https://doi.org/10.1038/ncomms10503.

91. Hua, R., Wang, X., Chen, X., Wang, X., Huang, P., Li, P., Mei, W., and Li, H. (2018). Calretinin neurons in the midline Thalamus modulate starvation-induced arousal. Curr. Biol. *28*, 3948–3959.e4. https://doi.org/10.1016/j.cub.2018.11.020.

92. Tseng, W.T., Yen, C.T., and Tsai, M.L. (2011). A bundled microwire array for long-term chronic single-unit recording in deep brain regions of behaving rats. J. Neurosci. Methods *201*, 368–376. https://doi.org/10.1016/j.jneumeth.2011.08.028.

93. Varga, C., Golshani, P., and Soltesz, I. (2012). Frequency-invariant temporal ordering of interneuronal discharges during hippocampal oscillations in awake mice. Proc. Natl. Acad. Sci. USA *109*, E2726–E2734. https://doi.org/10.1073/pnas.1210929109.

Please cite this article in press as: Fan et al., Neural mechanism underlying depressive-like state associated with social status loss, Cell (2023), https://doi.org/10.1016/j.cell.2022.12.033

STAR★METHODS

KEY RESOURCES TABLE

REAGENT or RESOURCE	SOURCE	IDENTIFIER
Antibodies		
Goat anti-rabbit Alexa Fluor 488	Thermo Fisher Scientific	Cat# A-11034; RRID:AB_2576217
Rabbit anti-c-fos	Synaptic Systems	Cat# 226008; RRID:AB_2891278
Bacterial and virus strains		
AAV2/9-CaMKIIa-GCaMP6s	Taitool Bioscience (Shanghai)	Cat# S0229-9-H20
AAV2/9-hSyn-eNpHR3.0-mCherry-WPRE-pA	Taitool Bioscience (Shanghai)	Cat# S0463-9
AAV2/9-CAG-hChR2 (H134R)-tdTomato	Taitool Bioscience (Shanghai)	Cat# S0168-9
AAV2/9-hSyn-mCherry-WPRE-pA	Taitool Bioscience (Shanghai)	Cat# S0238-9
AAV2/9-CAG-Flex-GCaMP6s-WPRE-pA	Taitool Bioscience (Shanghai)	Cat# S0354-9
AAV2/9-hSyn-ChrimsonR-tdTomato-WPRE-SV40pA	Taitool Bioscience (Shanghai)	Cat# S0459-9
AAV2/9-hSyn-Flex-ChrimsonR-mCherry-WPRE-pA	Taitool Bioscience (Shanghai)	Cat# S0739-9
AAV2/9-EF1a-DIO-eNpHR3.0-mCherry	OBIO	Cat# H4882
AAV2/2_{retro}-hSyn-Cre-WPRE-pA	Taitool Bioscience (Shanghai)	Cat# S0278-2R
Chemicals, peptides, and recombinant proteins		
Ketamine	Gutian Pharma Co.	H35020148
Experimental models: Organisms/strains		
C57BL/6J mice	SLAC Laboratory animal Shanghai	N/A
Software and algorithms		
OmniPlex neural recording data acquisition system	Plexon	https://plexon.com/products/omniplex-software
NeuroExplorer	Plexon	https://plexon.com/products/neuroexplorer
Offline sorter	Plexon	https://plexon.com/products/offline-sorter
MATLAB R2015b	MathWorks	https://www.mathworks.com/products/matlab.html
Prism	GraphPad Software	https://www.graphpad.com/scientific-software/prism
BORIS	Friard and Gamba[86]	http://www.boris.unito.it/
ImageJ	National Institutes of Health	https://imagej.nih.gov/ij/index.html
Analysis code	Zhang et al.[54]	https://zenodo.org/record/5591050
Any-maze software	Stoelting	https://stoeltingco.com/Neuroscience/ANY-maze
Other		
473nm and 589nm LED	Newdoon, Hangzhou	http://www.newdoon.com/cn/en/
Fiber photometry system	ThinkerTech, Nanjing	http://www.thinkerbiotech.com/

RESOURCE AVAILABILITY

Lead contact

Further information and requests for reagents should be directed to and will be fulfilled by the lead contact, Hailan Hu (huhailan@zju.edu.cn).

Materials availability

This study did not generate new unique reagents.

Data and code availability

- All data reported in this paper will be shared by the lead contact upon request.
- All code has been deposited at Zenodo: https://zenodo.org/record/5591050.
- Any additional information required to reanalyze the data reported in this paper is available from the lead contact upon request.

Please cite this article in press as: Fan et al., Neural mechanism underlying depressive-like state associated with social status loss, Cell (2023), https://doi.org/10.1016/j.cell.2022.12.033

EXPERIMENTAL MODEL AND SUBJECT DETAILS

All animal-related experimental procedures were under the guidelines of the Animal Care and Use Committee of the animal facility at Zhejiang University. We used adult male C57BL/6J strain mice at the age ranging from 8 to 16 weeks for most of the experiments. Mice for the behavioral tests (except SPT), immunohistochemistry, and fiber photometry were randomly group-housed as 4 in a cage, and mice for *in vivo* recording were singly housed to prevent electrodes from being destroyed by cagemates. All mice were kept in standard conditions (a 12-h light/dark cycle under standard food and water supplies).

METHOD DETAILS

All behavioral, optogenetics, recording and imaging experiments were replicated in multiple mice with similar results (see Table S1 for exact numbers of mice, trials and/ or units for each experiment). Sample sizes were selected based on similar behavior assays.

Behavioral assays

Tube test

The tube test was designed to measure social dominance as described previously.[34,36,37] For male mice, we used a 30-cm transparent tube with 30-mm inside diameter which allows only a single mouse to pass through. We first trained group-housed mice to go through the tube alone for 2 days. After training, mice were tested in pairs. Two mice were introduced at both ends and released as they meet in the middle of the tube. The trial was terminated when one mouse retreated with four paws out of the tube. This mouse was scored as "loser", and the other mouse was scored as "winner". The tube test ranks of each mouse were determined daily by the number of wins against all other cagemates. The rank was considered stable when all four cagemate mice maintained the same ranks for at least 4 consecutive days. For inter-cage comparison, rank1 mice were tested against all 4 mice from other cages. They mostly either won against all 4 mice or lost to the other rank1 but won against the rest 3 mice. The more dominant rank1 mice in the first category were used for the following tests and randomly assigned to the both forced loss and go-through-tube groups. When conducting inter-cage tube test after forced loss and go-through-tube procedure, the experimenters were not aware of the experience of the test mice.

Forced loss

After acquiring a stable tube test rank in groups of four mice, we randomly assigned rank1 mice to forced loss and control groups. We forced the rank1 mice to lose to their subordinate cagemates (rank2, 3 and 4) by blocking the subordinate's side of the tube. Because there was no way to back out, subordinates could only push forward against the previous rank1 to exit the tube (Video S1). The tube blocker was connected to a dynamometer, which measured the force generated by a subordinate mouse during retreat. The whole "forced loss" procedure contained 10 trials per day for 4 days. The duration and force of each forced loss trial were recorded. On the 5th day, tube test was performed normally without the blocker to check whether the rank of the original rank1 mice had dropped. Meanwhile, the cagemates of the forced-loss mice experienced the "forced win" procedure.

Natural loss and go-through-tube control groups

For controls of the forced loss, we have a naive group, a "go-through-tube" group and two "natural loss" groups. The naive group was mice without any extra experience other than tube tests with cagemates. The "go-through-tube" group was rank1 mice which went through the tube alone without encountering opponents for 10 trials per day for 4 days. The first "natural loss" group was rank1 mice which had experienced loss to three different rank1 mice of other cages in previous inter-cage tests. After such loss experience (3 trials daily for at least 4 days), these rank1 mice tended to retreat when facing the other three dominant rank1 mice even though they still won against their own cagemates. During the natural loss procedure, they were paired with the other three more dominant rank1 mice for 10 trials per day for 4 days. The second "natural loss" group was rank4 mice which had lost to their cagemates in previous inner-cage tests. During the natural loss procedure, they were paired with different cagemates for 10 trials per day for 4 days. These two "natural loss" groups showed no difference in score of depressive-like behaviors (Figure S2D), so their data were merged in Figures 2B and 2C. For the experiments in Figures 3, 4, and 5, we only used the rank1 mice losing to the familiar rank1s from other cages as the "natural loss" group.

Warm spot test

The warm spot test was applied as described.[40] A rectangular plastic test cage (28 cm × 20 cm) was put on ice to cool down its floor to 0 °C. In the cage, a round nest made of cardboard was placed at one corner, with a small heating coil underneath to warm the local temperature to 25∼27 °C. Temperatures were monitored by an infrared thermometer. The nest is 5 cm in diameter and 1.5 cm in height, allowing only one adult mouse to lie down. A cage of four mice was first placed in a cage on ice without a warm nest for 30 min to cool down, and then transferred to the test cage where they competed for the nest on the warm spot. Behaviors of the four mice in the test cage were videotaped for 20 min. For scoring occupation duration of the warm spot, the experimenter was not aware of the experience or ranks of the mice when annotating the behaviors. BORIS[86] was used to annotate the timestamp of squeezing in and being squeezed out of nest for each mouse, and the sum of the intervals in between was used to calculate the total duration. In the case when two mice stacked on top of each other, occupation duration was counted for both mice.

Please cite this article in press as: Fan et al., Neural mechanism underlying depressive-like state associated with social status loss, Cell (2023), https://doi.org/10.1016/j.cell.2022.12.033

Homecage behavior analysis

To analyze behaviors in the homecage, the test animals were put back to their homecage immediately after behavioral manipulations (regular tube test, natural loss and forced loss), and monitored for 15 min by an infrared camera. BORIS[86] was used to mark the behaviors in the video. "Staying alone" was defined as no movement in one place for more than 3 seconds, with no exploration or feeding behavior, and with no cagemates around within 10 cm distance; "fight" was defined as a series of behaviors between the subject mouse and cagemates, including bite, tumbling, attack and suchlike aggressive behaviors.[87]

Forced swim test (FST)

FST was performed as previously described.[88,89] Cylinders of 12-cm diameter and 25-cm height which was filled with warm water (23∼25 °C, mostly 24 °C) for the test. Under normal light, mice were gently and individually released into the water of 15-cm depth, which prevents their tails or hind legs from touching the bottom of the cylinder. The entire test lasted for 6 min. A camera was set at the side of the cylinder to record the behaviors. Before the test, the cage numbers were blinded by an experimenter who was not involved in the project. The videos were also blinded. The duration of immobility during the last 4 min after mice being introduced into the water and the latency to the first immobility was analyzed by one or two experimenters who were not aware of the experience of the mice. Immobility was defined by animals remaining floating or motionless with only small and necessary movements for keeping balance.

Sucrose preference test (SPT)

SPT was conducted as previously described,[32,33,88] taking 2 or 4 days of habituation, 1-day water-deprived phase and 1-day test phase. Mice were singly housed with blinded cage number to make sure that the experimenters were not aware of the experience of the test mice. Then, mice were habituated to two bottles of drinking water for the first one or two days and then with two bottles of 1% sucrose for one or two days. After habituation, the preference for any specific bottle was checked. Only mice without basal preference (between 25-75%) were used. Mice with basal preference of one bottle on the last day of habituation (below 25% or above 75%) were excluded. Mice were then water-deprived for 24 hr. In the test phase, mice were exposed to one bottle of water and one bottle of 1% sucrose for 2 hr in the dark phase, usually starting at 7:00 PM. The positions of 2 bottles were switched after 1hr. The sucrose preference was calculated as the average of consumption of sucrose/ total consumption of water and sucrose during the 2 hr.

Open field test (OFT)

Mice were individually placed in the center zone of a chamber (40 cm × 40 cm × 40.5 cm) with dim light for 10 min. Movement was tracked by a camera which was positioned directly above the arena and analyzed by Any-maze software (Stoelting). The total distance of each mouse traveled was analyzed.

Conditioned place aversion test (CPA)

The CPA protocol of losing was developed on the basis of a previously published protocol,[23] consisting of three phases: pre-test, acquisition and test. The CPA apparatus consists of two adjacent test chambers with different visual and somatosensory signals and one preparation chamber. During the 2-day pre-test, mice were individually placed into the preparation chamber and then allowed to shuttle between two test chambers freely for 15 min. The test chamber in which mice stayed longer was regarded as the preferred chamber, and the other chamber as the non-preferred chamber. During the acquisition phase, mice experienced a morning and an afternoon conditioning trial each day for two successive days. During the morning trial, mice were directly placed in the non-preferred chamber. During the afternoon trial, mice were placed and confined in the preferred chamber right after a specific experience (5 × "forced loss", 5 × "natural loss", 5 × "loss-to-stranger", or 5 × "go-through-tube"). Each conditioning trial lasted for 30 min. The interval between two conditioning trials was at least 4 hr. Finally, in the test phase, we tested the place preference of each mouse during a 15-min exploration. The duration in each chamber was automatically analyzed by Any-maze software (Stoelting, Ireland). CPA scores were calculated (CPA scores = duration in the chamber paired with specific experience in the test phase on day 5 - duration in the same chamber in the 2nd day of pre-test).

Surgery and viral injection

AAV2/9-CaMKIIa-GCaMP6s (titre: 1.23 × 10^{13} vector genome (v. g.)/ml, dilution: 1: 5, 0.1 μl unilateral into LHb, Taitool Bioscience), AAV2/9-hSyn-eNpHR3.0-mCherry-WPRE-pA (titre: 1.76 × 10^{13} v. g./ml, dilution: 1: 8, 0.1 μl per side bilateral into LHb and 0.2 μl 0.1 μl per side bilateral into LH, Taitool Bioscience), AAV2/9-CAG-hChR2 (H134R)-tdTomato (titre: 1.32 × 10^{13} v. g./ml, dilution: 1: 5, 0.2 μl unilateral into mPFC, Taitool Bioscience), AAV2/9-hSyn-mCherry-WPRE-pA (titre: 2.49 × 10^{13} v. g./ml, dilution: 1: 5, 0.1 μl unilateral into LHb, 0.2 μl unilateral into mPFC, Taitool Bioscience), AAV2/2retro-hSyn-Cre-WPRE-pA (titre: 1.82 × 10^{13} v. g./ml, dilution: 1: 2, 0.1 μl unilateral into LHb, Taitool Bioscience), AAV2/9-CAG-Flex-GCaMP6s-WPRE-pA (titre: 1.66 × 10^{13} v. g.)/ml, dilution: 1: 5, 0.1 μl unilateral into LH and 0.2 μl unilateral into mPFC, Taitool Bioscience), AAV2/9-hSyn-ChrimsonR-tdTomato-WPRE-SV40pA (titre: 2.27 × 10^{13} v. g./ml, dilution: 1: 10, 0.1 μl unilateral into LH, Taitool Bioscience), AAV2/9-hSyn-Flex-ChrimsonR-mCherry-WPRE-pA (titre: 1.30 × 10^{13} v. g./ml, dilution: 1: 5, 0.2 μl unilateral into mPFC, Taitool Bioscience) , AAV2/9-EF1a-DIO-eNpHR3.0-mCherry (titre:1.33 × 10^{13} v. g./ml, dilution: 1: 10, 0.2 μl unilateral into mPFC, OBIO) were aliquoted and stored at −80 °C until use.

Mice were deeply anesthetized and head-fixed in a stereotactic frame (RWD Instruments). Virus (0.1 μl into per side of LHb, 0.2 μl into per side of mPFC and 0.1 μl into per side of LH) was injected into either the LHb (AP, - 1.72 mm from bregma; ML, ± 0.46 mm; DV, - 2.55 mm from the brain surface) or the mPFC (AP, + 2.43 mm from bregma; ML, ± 0.45 mm; DV, - 1.2 mm from the brain surface) or the LH (AP, - 0.90 mm from bregma; ML, ± 1.20 mm; DV, - 4.90 mm from the brain surface) by a pulled glass capillary with a pressure

Please cite this article in press as: Fan et al., Neural mechanism underlying depressive-like state associated with social status loss, Cell (2023), https://doi.org/10.1016/j.cell.2022.12.033

microinjector (Picospritzer III, Parker). At the end of the injection, the needle stayed for about 10 min before being withdrawn to prevent fluid from refluxing. For fiber-optic cannula implantation, a 200-μm optic fiber (Inper) was placed 300 μm above the center of the viral injection site and cemented onto the skull by dental acrylic. For bilateral inhibition and activation of the LHb neurons or LH-LHb pathway, optic fiber was implanted at - 1.72 mm AP, + 1.14 mm ML, - 2.35 mm DV, and angled at 15° from the vertical in the lateral direction.

After surgery and above 7-day recovery, tube tests were conducted again to make sure that rank of operated mice remained unchanged (Figures S6B and S7P).

Optogenetic manipulation in tube test and forced loss

Optogenetic manipulation of the tube test was performed as previously described.[37,40] A 12-mm slit was opened at the top of the tube to allow the passage of optogenetic fiber.

In the experiment of mPFC activation, rank1 mice were injected with ChR2 virus (AAV2/9 CaMKII-hChR2 (H134R)-mCherry) and implanted with optical fiber in their dmPFC and waited for 3 weeks for gene expression and recovery. After forced loss, these rank1 mice were habituated to fiber connection and tested against other cagemates wearing fake optic fiber to confirm their rank decline. Photostimulation was then applied (473 nm, 100 Hz, 9.9 ms per pulse, 4 pulses per second, average 4.0 min) during the tube tests. Mice were tested against those with the closest rank using the low power of light at first and if there was no rank change, laser power was gradually dialed up. A rank increase was scored if mice won against the same opponent from both sides of the tube. We then repeated the light-stimulated winning for a total of 10 times. After the photostimulation day, mice were tested again to check whether the new ranks were sustained.

In the LHb or LH-LHb inhibition experiments, rank1 mice were bilaterally injected with AAV2/9-hSyn-eNpHR3.0-mCherry-WPRE-pA in the LHb or LH and implanted with optical fibers in their LHb. Light was turned on (constant at 589 nm, averaging 3.84 +/- 0.51 mw) right before the mice entered the tube of the first trial, kept it on throughout the 10 forced trials and terminated after 10 trials were completed, which averaged 21.9+/-14.7 min. Mice of the control group went through the same procedure but expressed mCherry instead of NpHR. The protocol of inhibition of mPFC-LHb pathway during forced loss is identical to the above except that AAV2/2retro-hSyn-Cre-WPRE-pA and AAV2/9-EF1a-DIO-eNpHR3.0-mCherry virus were expressed in the LHb and mPFC respectively. Cre-dependent NpHR was used to restrict the viral expression within the LHb since mPFC also projects to the MD and PHb, which are in close proximity to the LHb.

For activation of LHb during tube test, we used two methods: 40 Hz activation of the LHb and 40 Hz activation of LH terminals. All 4 cagemate mice were unilaterally infected with AAV2/9-hSyn-ChrimsonR-tdTomato-WPRE-SV40pA in the LHb or LH. Optical fibers were unilaterally implanted in their LHb. Briefly, for activation of LHb neurons, 633 nm yellow light stimulation (40 Hz, 2 ms per pulse, averaging 2.6 +/- 1.9 mW) was delivered right after the mice encountered the opponent in the middle of the tube and turned off after one mouse exited the tube. For activation of LH-LHb pathway, 633 nm red-light pulses (40 Hz, 5 pulses per second, 2 ms per pulse) were delivered at LH terminals in the LHb during tube test. The protocol of activation of mPFC-LHb pathway during tube test is identical to that of LH-LHb activation except that AAV2/2retro-hSyn-Cre-WPRE-pA and AAV2/9-hSyn-Flex-ChrimsonR-mCherry were expressed in the LHb and mPFC respectively.

Systemic ketamine administration

Ketamine (Gutian Pharma Co.) was dissolved in 0.9% saline, diluted to 1 mg/ml, and administered intraperitoneally (10 mg/kg, i.p.). Animals were assigned randomly to the saline and ketamine injection groups, and used for behavioral testing (FST and SPT) 1 hr after drug injection. Tube test rank was checked 24 hr after drug injection.

Fiber photometry recording

The fiber photometry was performed as previously described.[20] The fiber photometry system (Thinker Tech Nanjing Biotech Co., Ltd.) allowed delivery of a beam of 488 nm laser light toward the target brain area to excite and record green fluorescent signals of GCaMP. To slow the GCaMP bleaching, the laser intensity was adjusted to a low level (40 μw) at the tip of optic fiber and the sampling frequency was set to 50 or 100 Hz. To synchronize the video and the recording, the integrated laser system simultaneously sent a light pulse to the video and an electrical pulse to the recording setup. Behaviors were recorded by a camera set aside of the tube and annotated as previously described[40] by BORIS[86] for further analysis. Briefly, "push" was characterized by one mouse shoving its head under the opponent and pushing forward; "resistance" was when the mouse held on to its territory when being pushed by its opponent, often with its head being pushed up; "retreat" was defined as walking backwards voluntarily without being pushed ("voluntary retreat"), or after being pushed ("passive retreat"). "Out" was defined as the mouse left the tube with all four paws out.

Data were analyzed by the codes (e. g. OpSignal, from Thinker Tech Nanjing Biotech Co., Ltd.) based on MATLAB. The fluorescence responses were indicated by delta-F/F_0 (calculated as (F-F_0)/ F_0) and binned at 10 or 20 ms. F_0 is the baseline average fluorescence signals in a 1-second-long period prior to the onset of a behavioral epoch. The normalized area under curve was calculated as the sum of fluorescence changes during the behavioral epoch divided by the duration of the behavioral epoch. The normalized area under curve of "out" was calculated as the sum of the fluorescence during 3 s after out onset divided by 3 s. Delta-F/F_0 are presented as heatmaps and also as average plots with a shaded area indicating the SEM. Permutation test was applied to analyze the statistical significance of the fluorescence response to the behaviors, as previously reported.[90] Briefly, for each time point, a set of

Please cite this article in press as: Fan et al., Neural mechanism underlying depressive-like state associated with social status loss, Cell (2023), https://doi.org/10.1016/j.cell.2022.12.033

p values were generated and superimposed on the average curves of the behavior-related fluorescence change. The thick red and blue lines indicated $p < 0.05$.

Electrophysiological Recordings

LHb brain slice preparation

Animals (13-week-old C57BL/6J mice) expressing NpHR were used for in vitro recording. The protocol of LHb brain slice preparation was as described previously.[49]

In vitro *electrophysiological recording*

For LHb neuron recordings, we used whole-cell patch-clamp to measure the neuronal activity and resting membrane potential (RMP), as previously described.[32] To test the effects of NpHR on RMP and neuron activities, light was delivered constantly at 589 nm, 5-mW intensity on NpHR-expressing neurons. Current-clamp recording was used to measure RMP which was determined at the silent period of neuronal activity in both light on and off trials. For NpHR inhibition, firing rate of each neuron was analyzed under current injection in both light on and off trials. The injected currents ranging from 40 pA to 180 pA to induce firing were the same in both light-on and -off trials.

In vivo *electrophysiological recording*

Single-unit recording was performed as previously described.[40,91,92] Briefly, a home-made microdrive array consisted of 16 platiniridium single electrodes (impedance 500-800 kΩ, California fine wire). During surgery, electrodes were implanted in the LHb (ML, ± 0.46 mm; AP, - 1.72 mm from bregma; DV, - 2.44 mm from the brain surface) of rank1 mice. Silver wires with two screws were attached to the skull as ground. The procedure of surgery was similar to fiber-optic cannula implantation (see above).

After the surgery, mice were assigned randomly to natural loss and forced loss groups. For the protection of electrodes, mice were single-housed and handled daily. 5 days after surgery, mice were put in tube tests daily with its electrodes connected to the recording headstage to get habituated to the recording procedure for about 2∼3 days. When tested for rank position after the single house and before the recording experiment, they remained at the rank1 position (Figure S5A). The force and duration of forced loss procedure was similar to rank1 mice from group-house condition (Figure S5B). They were able to be forced to lose to lower-ranked mice (Figure S5C). There was no obvious sign of aggressive interaction in the tube tests. During recording, wideband electronic signals (0.05-8000 Hz) were recorded by a neural recording system (Plexon Inc.) and digitized at 40 kHz with a gain of 5000 ×. Spontaneous spiking signals were band-pass filtered between 300 and 8000 Hz. A single channel without a detectable unit or common median reference (CMR) was assigned as a digital reference. Data were recorded in two 15-min sessions (before and 30 min after behaviors) and throughout the whole behavioral process. The video recording was also conducted simultaneously to get a side view of the tube at 25 frames per second. A light pulse with an electrical pulse was sent to the video and recording setup at the same time to synchronize the timeline of the video and electrophysiological recording. For recording after the 4-day forced loss/ natural loss procedure, data were recorded for 15 min after 30-min adaptation of headstage connection. The microdrive can lower the electrodes in the steps of 62 μm to record units of different Z-axis locations, which were verified at the end of each experiment (Figure 5B).

For recording of the dmPFC neurons while activating the LHb, we expressed AAV2/9-hSyn-ChrimsonR-tdTomato in the LHb for 2 weeks, and then implanted electrodes in the dmPFC and an optic fiber above the LHb. The recorded mice were free-moving during recording. 633 nm red light stimulation (40 Hz, 2 ms per pulse, averaging 0.85 +/- 0.42 mW, 60 s) was applied for LHb activation.

Spike sorting and data analysis

Data were analyzed as previously described.[32,91] Briefly, every single unit was identified by threshold crossing and two types of principal components by using Offline Sorter (Plexon Inc.). Waveforms with inter-spike intervals (ISIs) more than the refractory period (1 ms) were included. The signal-to-noise ratio of every used unit should be larger than 2. To ensure that no unit was discriminated against more than once on different channels, we plotted the cross-correlation histograms between every two units. Only one of the two units was kept for further analysis if one unit presented a peak of activity at a time that the other fired. For recording of the dmPFC neurons, units were further classified as the pPYR and pIN based on the trough-to-peak duration. A unit with > 400 μs of trough-to-peak duration was classified as pPYR neuron and with ≤400 μs of trough-to-peak duration was classified as pIN.[54,55,93]

All bursts were identified as a cluster of spikes starting with a maximal ISI of 20 ms, ending with a maximal of ISI of 50 ms, with intra-burst interval of 50 ms at least.[32] The minimum number of spikes in a burst was set at 2. The tonic firing was identified as the spikes with ISI larger than 50 ms. Bursts per minute, the percentage of spikes in bursts, mean frequency were analyzed by Neuroexplorer4 (Plexon Inc.). Bursting spike frequency was calculated as the percentage of spikes in bursts × mean frequency. Tonic spike frequency was calculated as (1- the percentage of spikes in bursts) × mean frequency. During the 10 trials of forced loss or natural loss, the baseline data were collected for about 1∼3 min before the 1st trial (when test mouse was outside its homecage). Neural activities, including bursts per minute, bursting spike per second and mean firing frequency, in between two consecutive trials were analyzed and normalized by the baseline.

For recording the dmPFC neurons during LHb activation, the PSTH was estimated by the raster plot, and then standardized to report the light-induced neuronal response. We then transformed the firing rates (FR) into z scores by subtracting the mean firing rates and being divided by the standard deviation of baseline activity of 60-s periods before the light pulses. Change index was calculated as $(FR_{light\ on} - FR_{light\ off}/\ FR_{light\ on} + FR_{light\ off})$. To identify units that significantly respond during light-on periods, we used Wilcoxon signed-rank test to compare mean firing rate of the 60-s light-on period with the 60-s baseline period.

Please cite this article in press as: Fan et al., Neural mechanism underlying depressive-like state associated with social status loss, Cell (2023), https://doi.org/10.1016/j.cell.2022.12.033

c-Fos Immunohistochemistry staining and counting

Immunohistochemistry for c-Fos was conducted as previously described.[45–47] After behavioral manipulation, mice were monitored manually for 2 hr at homecage to ensure that there were no fights within the group. Then, mice were deeply anesthetized with 1% pentobarbital sodium and perfused transcardially with 0.1 M phosphate buffer saline (PBS, pH = 7.4) followed by 4% paraformaldehyde in PBS. Brains were removed and postfixed overnight and dehydrated in 30% sucrose in PBS. Coronal brain sections (40 μm) were serially cut and divided for 6 interleaved sets. The brain sections were incubated with the rabbit polyclonal c-Fos antibody (1:5000, SYSY) at 4 °C overnight. The protein signals were visualized through the Alexa Fluor 488 after blinding with the goat anti-rabbit secondary antibody (1:1000, Thermo Fisher Scientific) for 2 hr at 24∼28 °C. Investigators were blind to group allocation when counting c-Fos$^+$ cells. The number of c-Fos$^+$ cells in the LHb (from bregma: -0.94 mm to -2.18 mm) is the average of one set of brain slices.

QUANTIFICATION AND STATISTICAL ANALYSIS

All data are shown as mean ± SEM. Statistical analyses were done with Prism 6 (GraphPad) or MATLAB. The data were analyzed by Student's test for Gaussian distributions, while Mann-Whitney test for non-Gaussian distributions. Results were considered statistically significant when the P value < 0.05. More details are provided in the Table S1.

CellPress

Supplemental figures

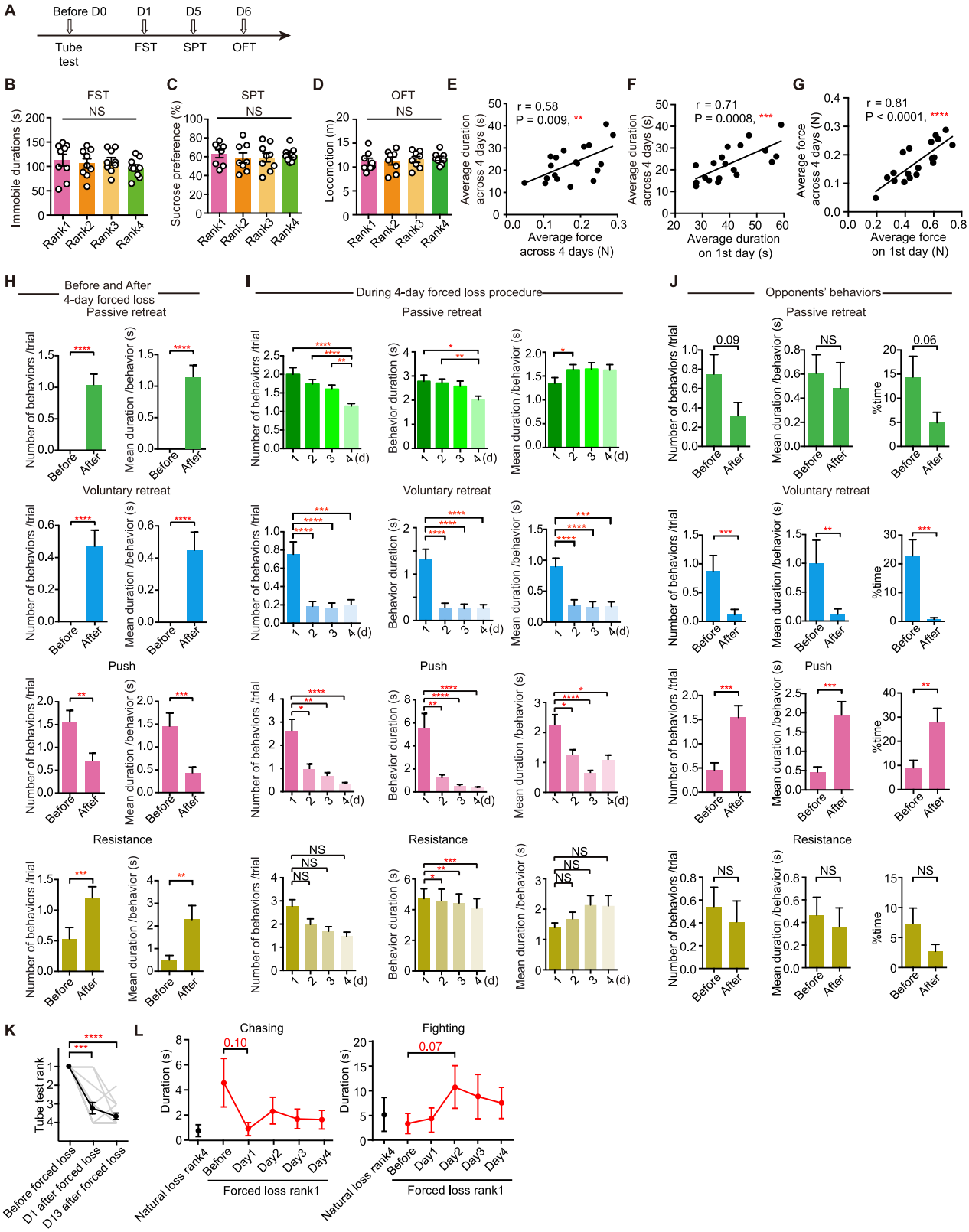

(legend on next page)

Figure S1. Other behavioral results, related to Figure 1

(A) Experimental schedule. After a stable rank was derived in the tube test for a cage of four mice, we sequentially performed the FST, SPT, and OFT on mice of different ranks.

(B–D) Immobility in the FST (B), sucrose preference in the SPT (C), and locomotion in the OFT (D) of mice of different ranks. n = 9, 9, 9, 9 mice in the FST; 8, 8, 9, 9 mice in the SPT; and 8, 8, 8, 8 mice in the OFT for mice of rank 1–4, respectively. Mann-Whitney test.

(E–G) Scatterplots showing the correlation between average force and average duration generated by opponent mice across 4 days (E), average duration on 1st day and average duration across 4 days (F), and average force on 1st day and average force across 4 days (G) during the "forced loss" paradigm. n = 19, Pearson correlation coefficients.

(H and I) Number of behaviors per trial, mean duration per behavior, and duration of behavior per trial that the original rank1 mice displayed before, after, and during the "forced loss" paradigm. Behaviors include passive retreat, voluntary retreat, push, and resistance. (I) Note that there are generally more behaviors on Day 1 because tube test durations are much longer on Day 1. n = 10 mice, 30 trials for before and after; n = 7 mice, 70 trials per day for during the forced loss. Mann-Whitney test.

(J) Number of behaviors per trial, mean duration per behavior, and percentage of time from meet to out that the opponent cagemates displayed before and after forced win against the original rank1 mice. n = 11, 8 mice, 24, 22 trials, Mann-Whitney test.

(K) Tube test ranks of mice before, 1st day, and 13 days after the forced loss procedure. Gray lines, rank change of individual animals. n = 14 cages, Wilcoxon signed-rank test.

(L) Chasing and fighting behaviors in the homecage after natural loss and 4-day forced loss. n = 23 for each condition, p = 0.10 for before forced loss versus after day 1 of forced loss, Wilcoxon signed-rank test; p = 0.07 for before forced loss versus after day 2 of forced loss, Wilcoxon signed-rank test.

****p < 0.0001; ***p < 0.001; **p < 0.01; *p < 0.05; ns, not significant. Data are represented as mean ± SEM.

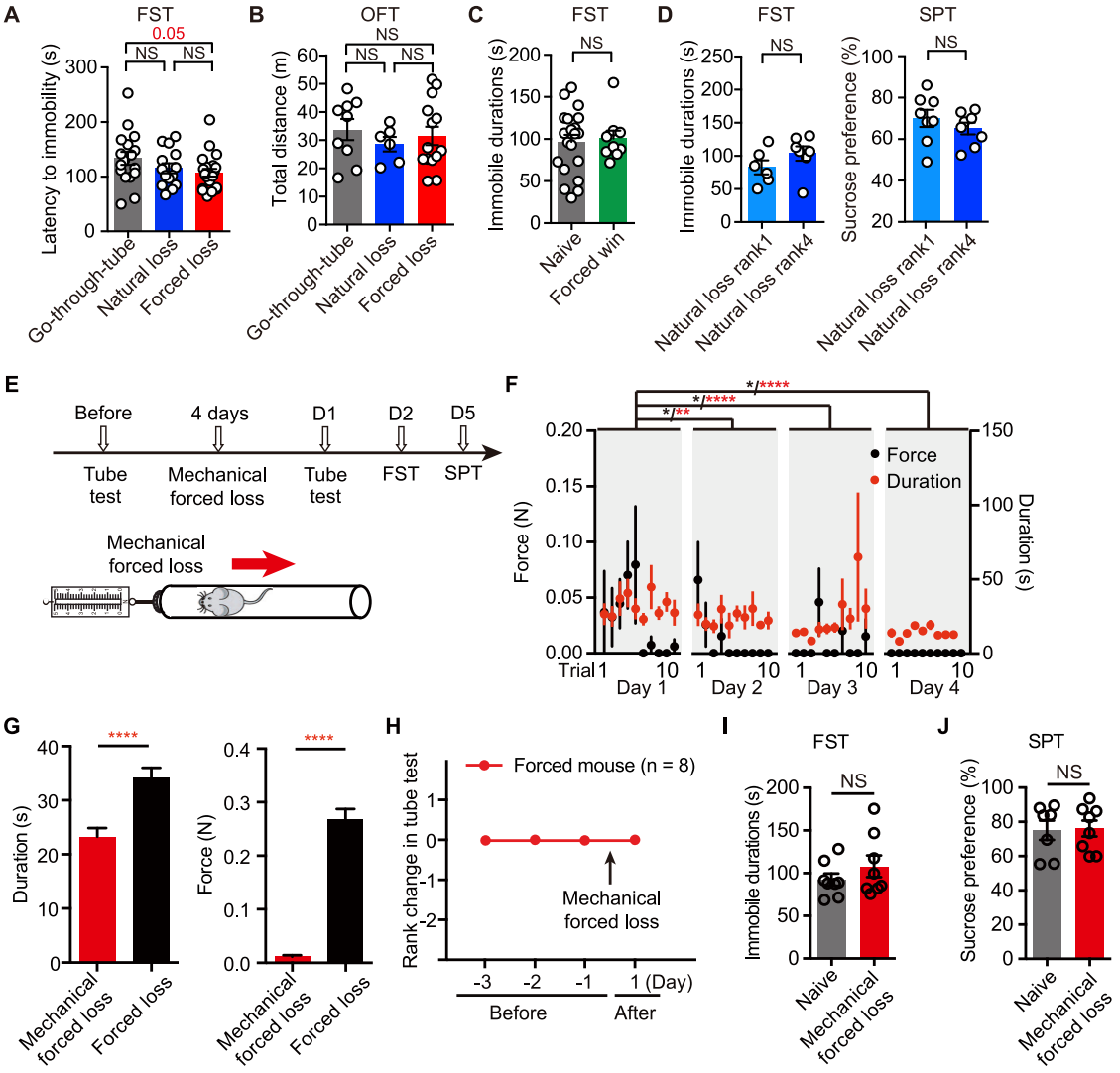

Figure S2. Other behavioral results, related to Figure 2

(A and B) Latency to immobility in the FST (A, n = 17, 14, 21) and total distance in the OFT (B, n = 9, 6, 14) conducted on the 2nd day after the go-through-tube, natural loss, and forced loss procedures. Two-tailed unpaired t test.

(C) Immobility in the FST conducted on the 2nd day in the naive control and forced win group (opponent mice in the forced loss procedure). Forced win experiments were performed simultaneously with the forced loss experiments, thus share the same control in Figure 2B. n = 20, 9. Two-tailed unpaired t test.

(D) Immobility in the FST (left, n = 6, 7) and sucrose preference in the SPT (right, n = 8, 8) after natural loss in rank1 and rank4 mice. Two-tailed unpaired t test.

(E) Experimental paradigm for behavioral tests (top) and schematic illustration (bottom) of mechanical forced loss.

(F) Scatterplot showing average forces (black dots) and duration (red dots) of each trial of the mechanical forced loss procedure. n = 8 mice, Two-tailed unpaired t test.

(G) Comparison of duration (left) and force (right) during mechanical forced loss and social forced loss against subordinate mice. n = 320 and 429 trials, left. n = 320 and 413, right. Two-tailed unpaired t test.

(H) Daily tube test results of mice before and after the 4-day mechanical forced loss procedure. n = 8 mice.

(I) Immobility duration in the FST in naive control and mechanical forced loss group (n = 8, 8). Two-tailed unpaired t test.

(J) Sucrose preference in the SPT in naive control and mechanical forced loss group (n = 7, 8). Two-tailed unpaired t test.

****p < 0.0001; **p < 0.01; *p < 0.05; ns, not significant. Data are represented as mean ± SEM.

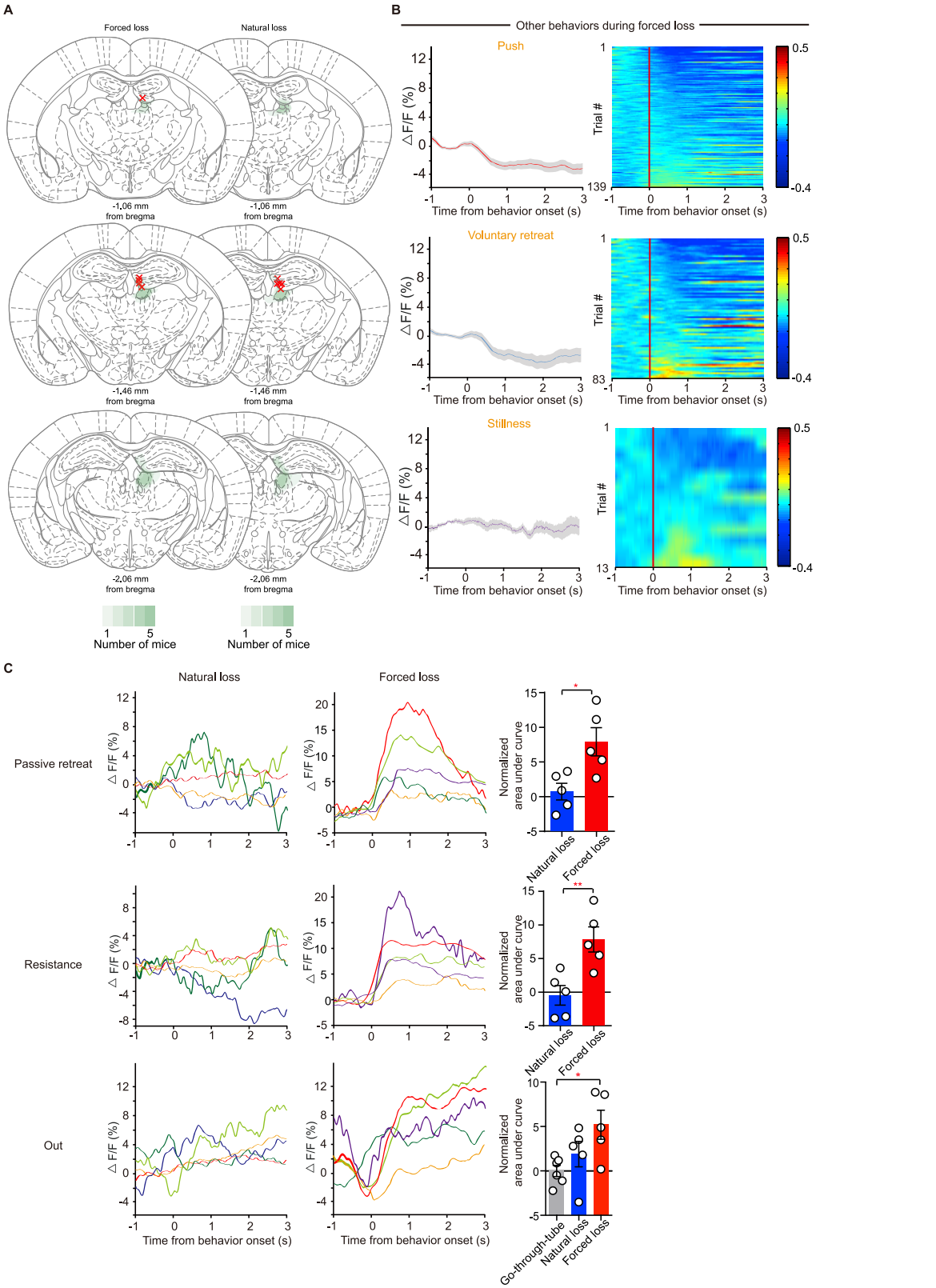

(legend on next page)

Figure S3. Fiber photometry of LHb during forced loss and natural loss, related to Figure 4

(A) Schematic of viral expression and optic fiber implantation in LHb for fiber photometry experiments. Green patterns represent the viral targeting area; red crosses represent the location of fiber.

(B) Averaged PSTHs (left) and heatmap representations (right) of the delta F/ F ratio of calcium signals aligned to the same behaviors (up, push; middle, voluntary retreat; and bottom, stillness) during day 1 of the forced loss.

(C) Averaged PSTHs of the delta F/ F ratio of calcium signals of individual animal aligned to the same behavioral epoch (up, passive retreat; middle, resistance; and bottom, out) during day 1 of natural loss (left) and forced loss (middle). Normalized average under curve (AUC) of LHb calcium signals of individual animals during different epochs (right). n = 6, 5, 5 mice for go-through-tube, natural loss, and forced loss, Mann-Whitney test.

**$p < 0.01$; *$p < 0.05$; ns, not significant. Data are represented as mean ± SEM.

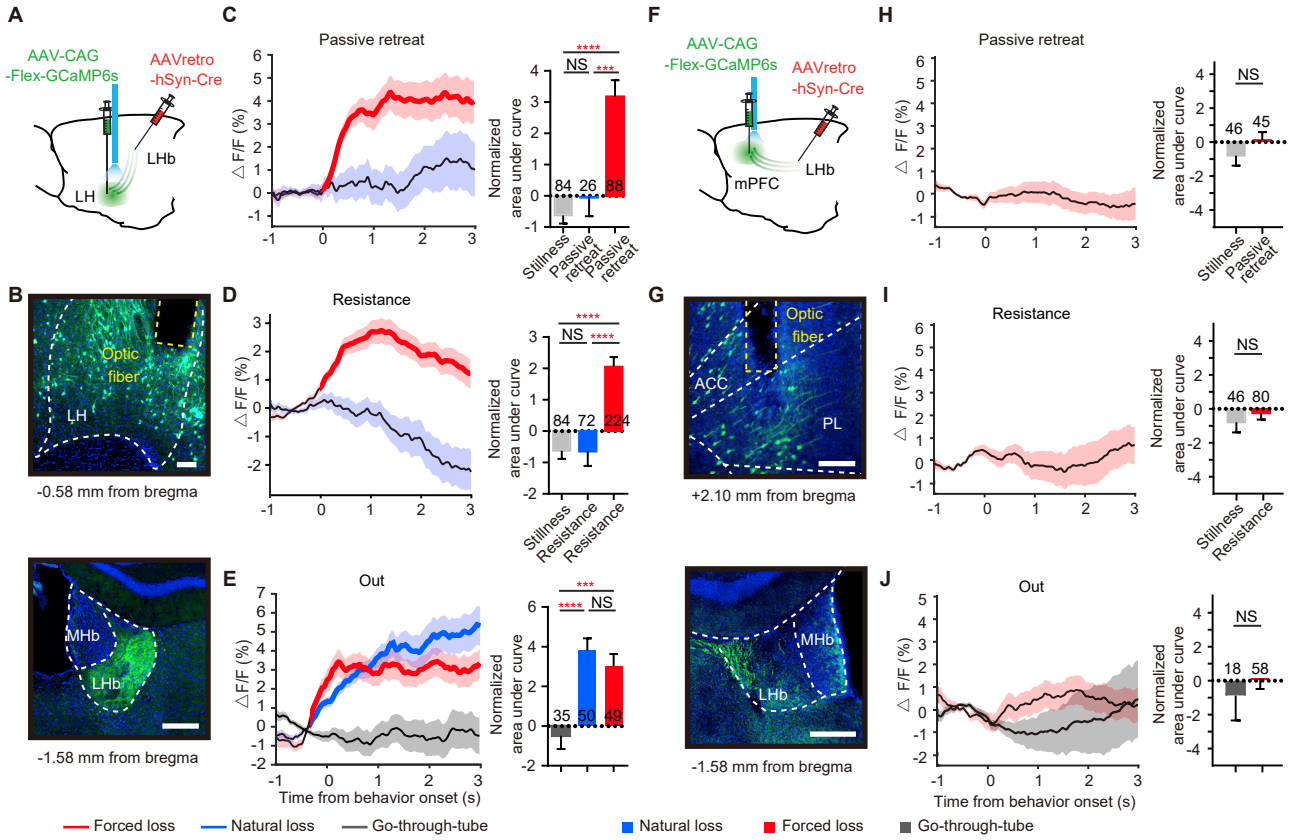

Figure S4. Fiber photometry of LH-LHb pathway during forced loss and natural loss, related to Figure 4

(A) Schematic illustration of the viral injection site and optic fiber placement in the LH and LHb.

(B) An example of GCaMP6s expression in LHb-projecting neurons of LH (top) and GCaMP6s labeled LH fibers in the LHb (bottom). Green, GCaMP6s; blue, Hoechst. Scale bars, 200 μm.

(C–E) Averaged PSTH (left) and normalized AUC (right) of the delta F/F ratio of calcium signals in the LH-LHb terminals aligned to various detailed behavioral epochs (C, passive retreat; D, resistance; E, out) during day 1 of forced loss and natural loss (n = 5, 5 mice). Left, thick black lines indicate the mean. Colored shaded areas indicate the SEM. Red or blue segments indicate statistically significant increases from the baseline ($p < 0.05$, multivariate permutation test). Right, Mann-Whitney test.

(F) Schematic illustration of the viral injection site and optic fiber placement in the mPFC and LHb.

(G) An example of GCaMP6s-expression in LHb-projecting neurons of mPFC (top) and GCaMP6s labeled mPFC fibers in the LHb (bottom). The boundary of which is outlined by the white dotted line. Note that the terminal projection from mPFC to LHb is much less than that from LH to LHb in (B). Green, GCaMP6s; blue, Hoechst. ACC, anterior cingulate; PL, prelimbic part of mPFC. Scale bars, 200 μm.

(H–J) Averaged PSTH (left) and normalized AUC (right) of the delta F/F ratio of calcium signals in the mPFC-LHb terminals aligned to various detailed behavioral epochs (H, passive retreat; I, resistance; J, out) during day 1 of forced loss (n = 5 mice). Mann-Whitney test.

****$p < 0.0001$; ***$p < 0.001$; ns, not significant. Data are represented as mean ± SEM.

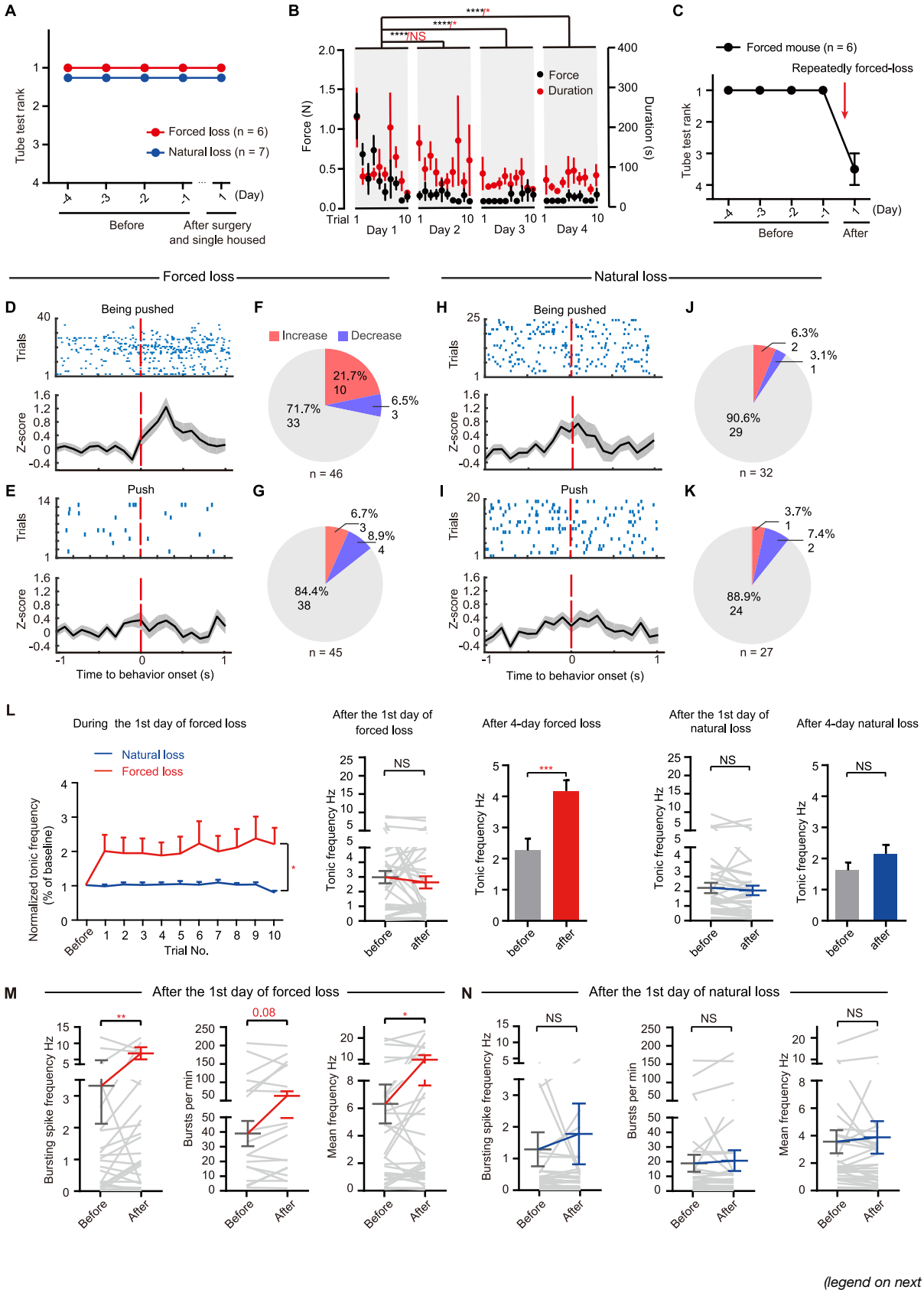

(legend on next page)

Figure S5. *In vivo* recording of LHb during forced loss and natural loss, related to Figure 5

(A) Tube test rank of mice before and after surgery of electrode implantation and single house (n = 6, 7). Red and blue points indicate the rank of mice in the forced loss and natural loss groups, respectively.

(B) Scatterplot showing average forces (black dots) and duration (red dots) of each forced loss trial during the 4-day procedure. n = 50 trials per day from 5 cages for day 1 versus days 2–4, respectively. Mann-Whitney test.

(C) Daily tube test results of mice before and after the 4-day forced loss procedure. n = 6 cages, Wilcoxon signed-rank test.

(D, E, H, and I) Raster plot of a representative unit (top), averaged PSTHs of the *Z* score of all recorded LHb neurons (bottom) aligned to being pushed by opponents (D and H) and push (E and I) during forced loss (D and E) or natural loss (H and I). Black lines indicate the mean; gray shaded areas indicate the SEM. Bin, 0.1 ms. n = 7, 6 mice.

(F, G, J, and K) Pie graphs show the percentage of units that have significantly higher (red), lower (blue), or unchanged (gray) firing rate during behavior epochs of forced loss (F and G) or natural loss (J and K). Paired t test. n = 7, 6 mice.

(L) Tonic firing frequency (left) of LHb neurons across 10 trials on the 1st day of forced loss (red, n = 33 units from 6 mice) and natural loss (blue, n = 42 units from 7 mice), normalized by the value before the first trial (left, two-way ANOVA). Tonic firing frequency of LHb neurons before and after the 1st day of forced loss (middle, Wilcoxon signed-rank test) and 4-day forced loss (right, Mann-Whitney test).

(M and N) Bursting spike frequency (left), bursts per min (middle), and mean frequency (right) of LHb neurons before and 30 min after 1st day of forced loss (M) and natural loss (N), recorded for 15 min at homecage. Wilcoxon signed-rank test.

****p < 0.0001; ***p < 0.001; **p < 0.01; *p < 0.05; ns, not significant. Data are represented as mean ± SEM.

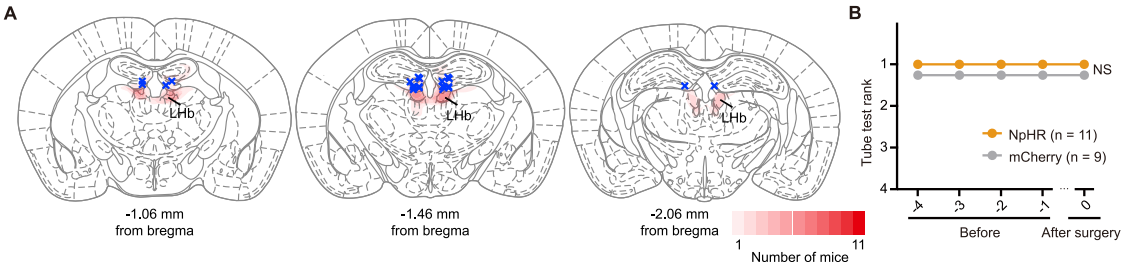

Figure S6. Viral targeting and fiber placement in the LHb, and tube test ranks before optogenetic manipulation, related to Figure 6

(A) Schematic of viral expression and optic fiber implantation in the LHb for inhibition. Red patterns represent the viral targeting area; blue crosses represent location of optic fiber.

(B) Tube test rank of mice expressing NpHR and mCherry in the LHb before and after surgery (n = 11, 9). Yellow points indicate rank of NpHR-expressing mice; gray points indicate rank of mCherry-expressing mice.

ns, not significant. Data are represented as mean ± SEM.

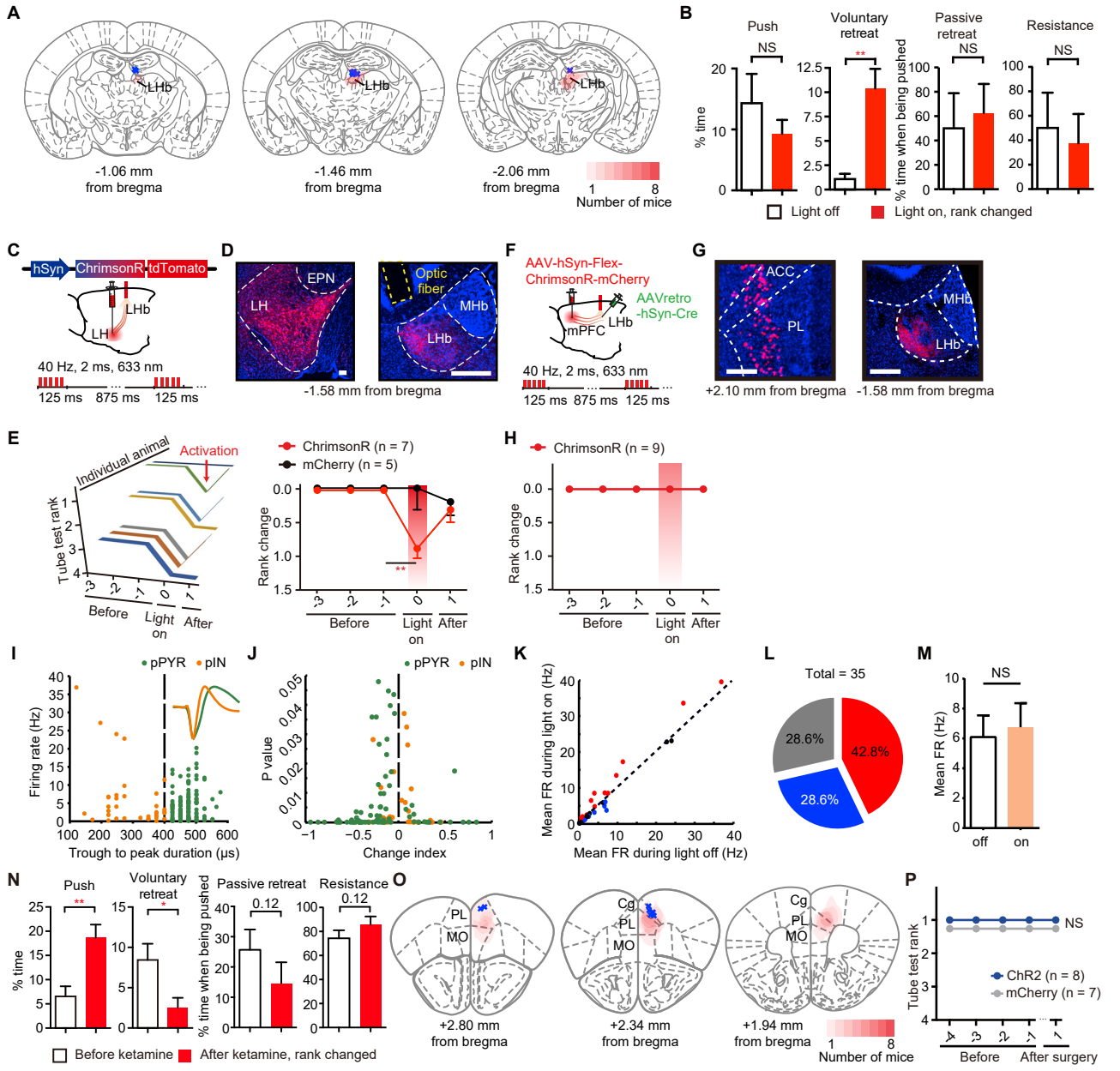

Figure S7. Other results of optogenetic manipulation, ketamine injection and *in vivo* recording of mPFC during LHb activation, related to Figure 7

(A) Schematic of viral expression and optic fiber implantation for activation of LHb. Red patterns represent the viral targeting area; blue crosses represent location of optic fiber.

(B) Percentage of time that mice displayed passive retreats and voluntary retreats during the whole test; percentage of time that mice displayed passive retreats and resistances when being pushed during light-off and light-on trials. n = 13, 16 for push; n = 13, 16 for voluntary retreat; n = 4, 4 for passive retreat; n = 4, 4 for resistance. Mann-Whitney test.

(C) Schematic illustrating the ChrimsonR viral construct and viral injection site for LH-LHb activation.

(D) An example of viral injection site in the LH (left) and terminal site in the LHb (right). Red, ChrimsonR; blue, Hoechst. Location of optic fiber placement is indicated by the yellow dotted line. Scale bars, 200 μm.

(E) Tube test rank of mice expressing ChrimsonR (left) and summary of tube test rank of all mice expressing ChrimsonR (red, right) and mCherry (black, right) under photostimulation. Light stimulation was delivered throughout the tube test at day 0. Wilcoxon signed-rank test.

(F) Schematic illustrating the ChrimsonR viral construct and viral injection site for mPFC-LHb activation.

(G) An example of viral injection site in the mPFC (left) and terminal site in the LHb (right). Red, ChrimsonR; blue, Hoechst. Location of optic fiber placement is indicated by the yellow dotted line. Scale bars, 200 μm.

(H) Summary of tube test rank of all mice expressing ChrimsonR (red) under photostimulation. Light stimulation was delivered throughout the tube test at day 0.

(legend continued on next page)

(I) Mean baseline firing rate (FR) plotted against peak-to-trough duration of all recorded units. Green circles indicate putative pyramidal neurons (pPYRs); orange circles indicate putative interneurons (pINs). Spike waveforms are shown at top right. n = 133, 35 for pPYRs and pINs.
(J) p value plotted against the change index of all significantly changed units ($p < 0.05$). Green circles indicate pPYRs; orange circles indicate pINs. n = 82, 25 for pPYRs and pINs. Paired t test.
(K) Scatterplots of mean FRs of pIN units (K) during light-off epoch against light-on epoch. Colored circles indicate units that show significant light-induced FR increase (red), decrease (blue), and no change (black). n = 35. Paired t test.
(L) Pie graphs showing the percentage of pIN units that have significantly higher (red), lower (blue), or unchanged (gray) FR during light stimulation.
(M) Mean FRs of pIN units during light-off and light-on epochs. n = 35. Wilcoxon signed-rank test.
(N) Percentage of time that mice displayed pushes and voluntary retreats during the whole test; percentage of time that mice displayed passive retreats and resistances when being pushed before and after ketamine i.p. injection. n = 21, 20 for push; 18, 16 for passive retreat; 21, 20 for voluntary retreat; 18, 16 for resistance. Mann-Whitney test.
(O) Schematic of viral expression and optic fiber implantation for activation of mPFC. Red patterns represent the viral targeting area; blue crosses represent location of optic fiber.
(P) Tube test rank of mice expressing ChR2 and mCherry in the mPFC before and after surgery (n = 8, 7). Blue points indicate the rank of ChR2-expressing mice; gray points indicate rank of mCherry-expressing mice.
**$p < 0.01$; *$p < 0.05$; ns, not significant. Data are represented as mean ± SEM.